

No 1041

# NATIONAL ADVISORY COMMITTEE FOR AERONAUTICS

TECHNICAL NOTE

No. 1041

EFFECT OF NORMAL PRESSURE ON STRENGTH OF  
AXIALLY LOADED SHEET-STRINGER PANELS

By A. E. McPherson, Samuel Levy, and George Zibritosky  
National Bureau of Standards



Washington  
July 1946

NATIONAL ADVISORY COMMITTEE FOR AERONAUTICS

TECHNICAL NOTE NO. 1041

EFFECT OF NORMAL PRESSURE ON STRENGTH OF

AXIALLY LOADED SHEET-STRINGER PANELS

By A. E. McPherson, Samuel Levy, and George Zibritosky

SUMMARY

Tests under combined axial load and normal pressure were made on 29 24S-T aluminum alloy sheet-stringer panels. The panels had lengths of 12 and 19 inches, widths of  $16\frac{3}{4}$  and  $24\frac{3}{4}$  inches, and sheet thicknesses of 0.025 and 0.051 inch. They were reinforced by extruded Z stringers spaced 4 inches between centers. The normal load on the sheet side of the panel was varied from 8 psi of vacuum to 16 psi of pressure.

Empirical formulas were derived for predicting the effect of normal pressure on the strain for buckling of sheet between stringers. The observed buckling strains were compared with theoretical values obtained in NACA Technical Note No. 949.

The axial load carried by the sheet was measured for all the panels. The measured axial load was compared with the theoretical axial load for sheet without normal load as given by Marguerre.

The maximum load and the mode of failure were observed for all the panels. The measured loads were compared with values obtained from the nomogram in NACA Technical Note No. 856 for flat panels of the same design without normal pressure. A simple formula was fitted to the data to describe the reduction of maximum axial load due to the presence of normal pressure.

## INTRODUCTION

An understanding of the effect of normal pressure on the strength of axially loaded sheet-stringer panels is important in the construction of airplane wings, pressurized cabins, and hull bottoms.

Experimental results on the effect of normal pressure on the critical compressive stress of sheet are limited to those presented in reference 1 for curved sheet specimens. Theoretical results on the effect of normal pressure on axially loaded sheet, having simply supported edges are presented in reference 2.

The tests described in this paper were made at the request of the National Advisory Committee for Aeronautics to provide additional experimental data and to derive empirical formulas for determining the buckling load, load carried after buckling, and ultimate load of sheet-stringer panels under combined axial load and normal pressure.

This investigation, conducted at the National Bureau of Standards, was sponsored by and conducted with the financial assistance of the National Advisory Committee for Aeronautics.

## DESCRIPTION OF SPECIMENS

The dimensions of the panels are given in table 1 and in figure 1. The stringers, the sheet, and the rivets were 24S-T aluminum alloy. The stringers were extrusions with a Z section having nominally the same dimensions for all the panels. Actually their cross-sectional area varied between 0.168 and 0.201 square inch. All the panels had a nominal rivet spacing of 20 times the sheet thickness and a nominal stringer spacing of 4 inches.

Panels 1 to 10 were tested over the widest range of normal pressures from 8 psi of vacuum to 16 psi of pressure, and were considered to be the basic set of panels. Panels 11 to 17 were included to determine the effect of a change in sheet thickness, panels 18 to 21 to determine the effect of a change in panel length, panels 22 to 25 to determine the effect of a change in both sheet thickness and panel length, and panels 26 to 29 to determine the effect of a change in both panel length and panel width.

The thickness of the sheet in the panels was taken as the average of a large number of measurements. The variation of sheet thickness in a given panel did not exceed 0.002 inch. The cross-sectional area of each panel was determined from its weight, density, and length after correcting for the weight of the rivet heads. This area differed by not more than 0.2 percent from the area obtained from cross-sectional dimensions.

### Mechanical Properties of Material

Tensile tests and single thickness compressive tests (reference 3) were made on specimens from the sheet used in the panels. The resulting compressive stress-strain curves are given in figure 2, and the mechanical properties in both tension and compression are given in table 2.

Compressive properties of the stringers were determined from compressive tests of 4-inch lengths of the stringer stock. One such test was made for each panel tested. The resulting family of compressive stress-strain curves and the median stress-strain curve are shown in figure 3. It was necessary to use the median curve of figure 3 for computations for all the panels since the correspondence between the numbering of the stringer samples and the numbering of the panels was not clear. Fortunately, except for 2 of the 29 curves, the difference from the median curve was less than 1 percent. For the remaining 2 curves the differences in modulus were 2 and 3 percent and the differences in yield strength (0.002 offset) were 5 and 6 percent.

### Preparation of Panels

The ends of each panel were ground flat and parallel. The panel length, weight, and cross-sectional dimensions were then determined.

### Test Fixture, Pressure on Sheet Side

A specimen set up for axial load combined with normal pressure on the sheet side is shown in figures 4 and 5. The specimen was set with its centroid at the center line of the machine. The axial load was applied to the panel through the ground end blocks C. The normal pressure was applied by means of the air cell B which was made of rubberized balloon cloth weighing about 0.04 pounds per square foot. The lateral

force developed by the pressure was transferred from the ends of the panel to the reaction bars A which were rigidly fastened to the end blocks C. Distortion of the sheet at the ends of the panel was prevented by casting Wood's metal D and E between the ends of the specimen and the reaction bars A and the back plate B, respectively. The reaction from the back plate B was carried to the end blocks by the lugs I. The intermediate rollers G permitted free motion of the heads relative to the back plate as the specimen shortened under load. This arrangement left the specimen practically free to deform under load and did not apply lateral forces to the testing machine.

#### Tests Fixture, Vacuum on Sheet Side

The setup for this condition of loading is shown in figure 6. In this case the reaction bars A were relocated on the end blocks so that the lateral force was carried directly by the sheet. The Wood's metal D prevented the stringers from rotating and as in the previous case prevented distortion of the sheet at the end of the panel. The lateral force on the vacuum cell F was carried to the end block by direct connection at one end and by the roller G at the other. The gaps between the vacuum cell, the specimen, and the heads were sealed by a loose fold of rubberized cloth cemented as shown at H. Small leaks were sealed with hot beeswax.

#### Test Fixture, No Pressure

The procedure for tests with no pressure was identical with that used for the pressure tests except that no cell was employed.

#### Pressure equipment

The systems for applying pressure and vacuum were equipped with regulator valves which maintained the desired pressure. Pressure and vacuum were measured by means of a mercury manometer calibrated in pounds per square inch.

#### Loading

When loading the panel, the ratio of axial load to normal pressure was always maintained sufficiently high to prevent tipping of the end of the panel on the steel loading block.

The loads for a particular panel were increased in small steps, keeping this ratio in mind. After the normal pressure reached a predetermined value, it was held constant and the panel was tested to failure by further increases in the axial load. In some of the panel tests the axial load was brought back to a low value with zero normal pressure at regular intervals to measure the permanent set in the stringers and in the sheet.

### Strain Measurements

Pairs of 2-inch Tuckerman strain gages were attached to the stringers of the panel. One gage of each pair was attached directly to the outstanding flange. The remaining gage of each pair was attached to the stringer flange joined to the sheet using the lever strain transfer described on page 4 of reference 4.

Wire strain gages of the SR-4 type were attached to the panels in addition to the Tuckerman gages when it was found that the Tuckerman gages could not be relied upon to give the increment in strain during buckling; the buckling was sometimes so violent that it unseated the Tuckerman strain gages.

Figure 4 shows one of the panels set up for test with the strain gages attached. Most of the SR-4 wire strain gages are on the under side of the stringers and therefore are not visible in the photograph.

Figure 7 shows the location of the strain gages on the stringer cross section. The strain  $\epsilon$  at the centroid of the stringer and the strain  $\epsilon'$  at the point of contact of the sheet and the stringer were computed from the measured strains on the assumption that the strain in the stringer varied linearly with the distance from the sheet. This assumption of linear strain variation was partially checked by attaching twelve SR-4 type A-1 wire strain gages to a single stringer of the type used in the panels and testing it under axial load. No deviation from linear strain variation across the section was observed until after severe bending at an axial stress of 40,000 psi.

### Uniformity of Strain

After mounting the panel in the testing machine, the strain was measured for small increments in axial load. At a load of about 10 percent of the expected maximum load, those panels which did not show a uniform strain distribution were removed from the testing machine and their ends were reground. They were then rechecked for uniformity of strain before testing. The maximum initial departure from uniformity in the panels as tested was 10 percent. Most of the panels showed considerably better uniformity.

### Buckling

The buckling of the sheet between stringers, the buckling of the sheet between rivets, and the twisting of the stringers was noted by frequent visual inspection as well as by the pop which in most cases accompanied buckling between stringers.

### Results of Test in Elastic Range

Panel 13 having 0.051-inch sheet with a 4-inch stringer spacing was loaded through a range of lateral pressures up to 7 psi and axial loads up to 30 kips in the elastic range to determine the effect of lateral pressure on the behavior of the sheet. The sheet in this panel buckled at an axial load of 17 kips with no lateral pressure. For each combination of axial load and lateral pressure the load was increased from a low load (axial load 4000 lb, lateral pressure zero) to the test load by two sequences. For the first sequence, the axial load was increased to the test axial load and then the lateral pressure was increased to the test lateral pressure; while for the second sequence, the order was reversed. This was done to determine the effect of sequence of loading. A permanent set reading was taken after each load reading to check that the elastic range as measured at the stringers had not been exceeded. The repetition of loading had no effect on the buckling load.

Buckling.— The development of the buckle pattern is indicated in figure 8. It is evident that the application of lateral pressure in some cases postponed buckling to higher axial loads. The changes in buckle pattern observed were mostly of the "snap" type. They were accompanied by a sudden decrease in the axial load of 50 to 100 pounds. The number of buckles increased with the axial load over a range of axial loads from 18 to 30 kips. The order of application of the loads had only a minor effect on the buckle pattern.

Sheet load.— In figure 9 is shown a plot of the sheet load as a function of lateral pressure and edge strain. The sheet load was computed from the measured stringer strains by subtracting the corresponding stringer loads from the total load. The sheet load for a given edge strain was changed less than 5 percent for a range of lateral pressures from 0 to 7 psi. The sequence of application of the loads in no case changed the sheet load by more than 2 percent.

In conclusion, the tests of panel 13 in the elastic range showed that lateral pressure from 0 to 7 psi had some influence on the buckling load (fig. 8), but changed the sheet load for a given edge strain less than 5 percent. The order of loading had a negligible effect on the sheet buckling and affected sheet load by less than 2 percent.

#### Results of Tests to Failure

Strains.— The load-strain graphs are shown in figures 10 to 38. The stringer strains are the strains  $\epsilon$  at the centroids of the stringers and the sheet strains are the strains  $\epsilon'$  in the extreme fiber of the stringer at the contact between stringer and sheet. The axial load at which the lateral pressure  $p$  was applied is indicated on the figures. Loads at which buckling of the sheet between stringers occurred are also given in the figures. The permanent set readings are given on some of the graphs.

An increase in axial load in general caused all the strains to increase by the same amount; while an increase in normal pressure in general caused a divergence between the strains read at the sheet and at the stringer centroid. The effect of pressure on the sheet side on the strains at the midlength was to increase the compressive strains at the sheet and decrease the compressive strains at the stringer centroid. Vacuum on the sheet side had the reverse effect.

Buckling.— The strains at which buckling of the sheet between stringers was first noticed are given in table 3. For most of the panels having lateral pressures of 1 psi or more, the buckling was of the "snap diaphragm" type. Two kinds of buckling of the sheet between stringers were observed. For the panels with relatively low pressures, the buckles extended from stringer to stringer just as for flat panels; while, for the panels with relatively high lateral pressure, some of the buckles extended only part way from stringer to stringer as in a thin-walled cylinder under axial load.



In figure 39 are shown at A, the lateral deflection of the unbuckled sheet; at B, a buckle extending from stringer to stringer; and at C, buckles extending only part way from stringer to stringer.

In addition to buckling of the sheet between stringers, there was buckling of the sheet between rivets. The nominal rivet spacing of 20 sheet thicknesses in the panels was chosen to give no buckling between rivets prior to failure in the absence of normal load. Only eight panels had buckles between rivets prior to failure. The buckling occurred nearly at failure. There was no indication that the normal load had appreciably reduced the strains for buckling between rivets.

Failure.— The maximum load and the average stress at failure are given in table 4. The average stress at failure varied from 19.9 ksi for panel 18 with 8 psi of vacuum, 0.025-inch sheet and 19-inch length to 32.7 ksi for panel 5 with 1/2 psi of vacuum, 0.025-inch sheet and 12-inch length. The average stress at failure for 0.051-inch panels was 7 percent less than for comparable 0.025-inch panels.

#### ANALYSIS

Buckling of sheet between stringers.— A theoretical discussion of the behavior of a simply supported, long, rectangular plate, length/width ratio 4, under combined axial load and normal pressure is given in reference 2. Figures 6 to 9 and tables I to IV of reference 2 indicate that buckling can occur as follows for such a plate:

$$\left. \begin{aligned} pb^4/Et^4 &= 0; & \epsilon_{cr} b^2/t^2 &= 3.84 \\ pb^4/Et^4 &= 2.40; & \epsilon_{cr} b^2/t^2 &= 4.1 \\ pb^4/Et^4 &= 12.02; & 7.32 < \epsilon_{cr} b^2/t^2 < 10.51 \\ pb^4/Et^4 &= 24.03; & 10.24 < \epsilon_{cr} b^2/t^2 < 15.42 \end{aligned} \right\} (1)$$

where

b      stringer spacing  
p      normal pressure  
t      sheet thickness  
 $\epsilon_{cr}$    critical buckling strain

The limiting values of critical strain when  $pb^4/Et^4 = 12.02$  and  $24.03$  indicate a range of values of  $\epsilon_{cr} b^2/t^2$  within which the sheet can be in stable equilibrium in either the buckled or unbuckled state. Above this range the sheet must be buckled and below it the sheet must be unbuckled.

In figures 40 and 41 are plotted the experimentally observed buckling strains for sheet between stringers as a function of lateral pressure. Figure 40 contains the data corresponding to all panels having a nominal sheet thickness of 0.025 inch while figure 41 contains the data for all panels having a nominal sheet thickness of 0.051 inch. It is evident from figures 40 and 41 that panel width and panel length as well as the direction of the lateral pressure (acting on stringer or sheet side) had negligible effect on the strain at which buckling of the sheet between stringers occurred while the magnitude of the lateral pressure had a large effect.

The theoretical buckling strains according to equation (1) are plotted as vertical bars in figures 40 and 41. They were computed by substituting in equations (1) the nominal values  $b = 4$  inches,  $t = 0.025$  inch,  $E = 10.6 \times 10^6$  psi for figure 40 and the nominal values  $b = 4$  inches,  $t = 0.051$  inch,  $E = 10.7 \times 10^6$  psi for figure 41. In comparing theoretical and measured buckling strains it must be remembered that equation (1) corresponds to simple support along the edges while the edge conditions in the test panels were intermediate between simple and clamped support.

The increase in edge restraint above simple support has opposite effects on the buckling strain of the sheet, depending on the magnitude of the lateral pressure. At very low pressures the sheet buckles as a flat plate at a strain which will increase with the amount of edge restraint. At sufficiently high pressures the buckling strain is determined principally by the transverse curvature which is produced by the "dishing in" of the sheet under lateral pressure. The dishing in and the transverse curvature are decreased with increasing edge restraint. Hence, at high pressures, a decrease in buckling strain with increase in edge restraint is expected.

The anomalous effect of edge restraint on buckling strain may be responsible in part for the fact that the experimental buckling strains in figures 40 and 41 for the panels with intermediate support are larger at low pressure than the theoretical buckling strains for simple support, while they are smaller at high pressures.

The anomalous effect is checked by the experimental fact that the buckling was first observed on interior bays for every one of the panels having more than 2 psi of pressure or vacuum while for the remaining panels buckling occurred in the edge bays first or all over at once. The edge stringers twisted, corresponding to an edge condition nearer to simple support, and made the dishing in of the edge bays deeper than that of the interior bays. For panel 12 this was checked by measuring lateral deflections due to pressure. It was found that the edge bays dished 37 percent more than the interior bays.

A quantitative measure of the anomalous effect can be obtained by fitting an empirical relation to the experimental buckling strains in figures 40 and 41. Such an empirical relation was obtained by noting from equations (1) that the critical strain ratio  $\epsilon_{cr} b^2/t^2$  should be some function of the pressure ratio  $pb^4/Et^4$ . In figures 40 and 41 are shown straight lines, faired through the data, corresponding to a linear relation between these variables. These straight lines are for the 0.025-inch sheet:

$$\epsilon_{cr} \frac{b^2}{t^2} = 7.0 + 0.062 \frac{pb^4}{Et^4} \quad (b/t = 160) \quad (2a)$$

and for the 0.051-inch sheet:

$$\epsilon_{cr} \frac{b^2}{t^2} = 4.5 + 0.16 \frac{pb^4}{Et^4} \quad (b/t = 78) \quad (2b)$$

The first term on the right-hand side of these equations corresponds to the case of no lateral pressure. Comparing this term with the theoretical value for a long plate with clamped edges and with simply supported edges (reference 7, pp. 604-607):

$$\epsilon_{cr} \frac{b^2}{t^2} = 6.4 \quad \text{clamped edges}$$

$$\epsilon_{cr} \frac{b^2}{t^2} = 3.7 \quad \text{simply supported edges}$$

shows that the 0.025-inch sheet in figure 40 approached a condition of rigid clamping at the stringer while the 0.051-inch sheet in figure 41 approached a condition of simple support.

The coefficient of the pressure term on the right-hand side of equations (2a), (2b) is about 160 percent larger for (2b), approaching simple support, than for (2a), approaching clamped support. In other words, the buckling strain for large pressures on these panels can be increased about 2.6 times by decreasing the edge restraint at the stringer from rigid clamping to simple support.

The effect of changing the thickness of sheet, with a given edge condition, is also brought out clearly by equations (2a), (2b). With increasing thickness the first term, corresponding to buckling at low pressure is increased; while the second term, corresponding to buckling at high pressure, is decreased. This accounts for the experimental fact, shown in figures 40 and 41, that the panels with the thin sheet, figure 40, were more stable at pressures above 8 psi than the panels with the heavy sheet in figure 41.

In applying equations (2a), (2b) it must be remembered that they are based on tests involving only one stringer spacing,  $b = 4$  inches, two sheet thicknesses,  $t = 0.025$  and 0.051 inch, and one type of stringer. The equations are not recommended for design outside of the range of variables involved in the test.

Sheet Load.— The sheet load per sheet bay  $P_{sh}$  was calculated by subtracting the load carried by the stringers from the applied load and dividing by the number of sheet bays. (No correction was made for the extra  $3/8$  inch of sheet beyond the rivet line of each edge stringer.) The load on each stringer was obtained from the strain at the stringer centroid, the compressive stress-strain curve (curve B, fig. 3), and the cross-sectional area of the stringer (table 1). The sheet load per sheet bay  $P_{sh}$ , so determined, is plotted in figures 42 to 48 against the sheet strain (strain at extreme fiber of the stringer at the contact between stringer and sheet). Figures 42, 43, 46, and 48 are for panels with 0.025-inch sheet; while figures 44, 45, and 47 are for panels with 0.051-inch sheet.

Figures 42 to 48 show that the effect of lateral pressure is much more pronounced for the 0.025-inch sheet than for the 0.051-inch sheet. The sheet load for a given edge strain is decreased by lateral pressure for strains less than the buckling strain with no lateral pressure, but is increased for strains somewhat greater than the buckling strain with no lateral pressure. Comparison of figures 42 to 48 with each other show that the sheet load per bay is unaffected by the over-all panel width, panel length, or direction of application of the normal load (i.e., pressure or vacuum).

A theoretical value of the sheet load for the case where the normal pressure is zero can be obtained from Marguerre's formula (reference 6, p. 12). According to this formula, in the elastic range the load per sheet bay  $P_{sh}$  carried by a sheet of thickness  $t$  between stringers with a spacing  $b$  at an edge strain  $\epsilon'$  is:

$$\left. \begin{aligned} P_{sh} &= btE \epsilon'; \quad \epsilon' < 3.64t^2/b^2 \\ P_{sh} &= btE \epsilon' \left( \frac{3.64t^2}{\epsilon' b^2} \right)^{1/3}; \quad \epsilon' > 3.64t^2/b^2 \end{aligned} \right\} \quad (3)$$

It is shown in reference 6 that Marguerre's formula gives values of sheet load that are from 8 percent more to 20 percent less, inside the elastic range, than measured values for panels similar to those of this report but without normal pressure.

The panels of this report with a nominal sheet thickness  $t = 0.025$  inch had an average Young's modulus of the sheet  $E = 10.6 \times 10^6$  psi and an average stringer spacing  $b = 4$  inches. For these panels, equations (3) reduce to

$$\left. \begin{aligned} P_{sh} &= 1.06 \times 10^6 \epsilon'; \quad \epsilon' < 0.000142 \\ P_{sh} &= 55320(\epsilon')^{2/3}; \quad \epsilon' > 0.000142 \end{aligned} \right\} \quad (4)$$

For the panels having a nominal sheet thickness  $t = 0.051$  inch, the average Young's modulus of the sheet was  $10.7 \times 10^6$  psi, and the stringer spacing was  $b = 4$  inches. For these panels, equations (4) reduce to

$$\left. \begin{aligned} P_{sh} &= 2.132 \times 10^6 \epsilon', & \epsilon' < 0.000592 \\ P_{sh} &= 183,600 (\epsilon')^{2/3}, & \epsilon' > 0.000592 \end{aligned} \right\} \quad (5)$$

Equations (4) and (5) are plotted in figures 42, 43, 46, 48 and 44, 45, 47, respectively. Comparison with the observed sheet loads in these figures shows that Marguerre's formula gives a conservative value of the sheet load regardless of pressure, except at loads below the buckling load for some of the panels carrying large lateral pressure. The measured sheet loads are in some cases considerably more than the 20 percent in excess of Marguerre's formula observed in reference 6 for panels without normal pressure. This indicates that Marguerre's formula may be conservative in the range between the buckling strain and failure by even more than 20 percent, particularly in the presence of normal pressure.

Failure.— The data in table 4 showing the effect of normal pressure on the average axial stress at failure are plotted in figures 49 to 53.

Normal load caused a small reduction (about 1/2 percent per psi) in the axial load at failure for the 12-inch panels (figs. 49 and 50) and a somewhat greater reduction (about 2 percent per psi) for the 19-inch panels (figs. 51 to 53). The direction of application of the normal load — that is, pressure or vacuum on the sheet side — has no effect on the magnitude of this reduction. The panels with 0.025-inch sheet (figs. 49, 51, and 53) show approximately the same reduction as the panels with 0.051-inch sheet.

In addition there is plotted in figures 49 to 53 an estimated stress at failure determined from the nomogram in figure 56 of reference 6 using average panel dimensions and a value of  $\sigma_{st}$  (stringer stress at failure) of 39 ksi for the 12-inch panels and 36 ksi for the 19-inch panels. The value of 36 ksi was chosen for 19-inch panels on the basis of unpublished tests.

The stress obtained from the nomogram agrees with the observed stresses within 6 percent for all the panels tested with a lateral pressure of 4 psi or less of normal load.

A simple correction to take account of the reduction of axial stress at failure due to normal load was derived on the assumption that the reduction would be proportional to the ratio of center deflection to length with only normal load acting. On this basis, the reduction for a particular type of stringer should be proportional to  $pb^3/EI$ , where  $p$  is the normal pressure,  $b$  is the stringer spacing,  $l$  is the length, and  $EI$  is the bending stiffness per bay. For the purposes of this simple correction,  $EI$  was taken as the bending stiffness of a single stringer with a single sheet bay attached and it was assumed that the sheet was fully effective. On this basis,

$$\frac{P}{A} = \left(\frac{P}{A}\right)_{\text{nomo}} \left[1 - k \frac{pb^3}{EI}\right] \quad (6)$$

where

$P/A$  average axial stress at failure

$(P/A)_{\text{nomo}}$  value of  $P/A$  determined from nomogram in reference 6

$k$  empirical constant to be determined from data

The value of  $k$  which gave the best fit to the data in figures 49 to 53 using  $EI = 478,000$  pound-inches square for 0.025-inch panels (figs. 49, 51, and 53) and  $EI = 583,000$  pound-inches square for the 0.051-inch panels (figs. 50 and 52) was  $k = 0.39$ . Formula (6) then becomes

$$\frac{P}{A} = \left(\frac{P}{A}\right)_{\text{nomo}} \left[1 - 0.39 \frac{pb^3}{EI}\right] \quad (7)$$

Equation (7) is plotted in figures 49 to 53 for comparison with the data. The failing stress of 27 of the 29 panels tested agree with equation (7) within 6 percent. The remaining two panels, 18 and 21 of figure 51, carried 8 psi of normal load and were 18 percent weaker and 9 percent stronger, respectively, than indicated by equation (7).

## CONCLUSIONS

In the elastic range, a panel with 0.051-inch sheet and 4-inch stringer spacing subjected to normal pressures from 0 to 7 psi showed some change in buckling load with normal pressure, but showed changes of less than 5 percent in the sheet load for a given edge strain, the order of loading (i.e., pressure or axial load first) had a negligible effect on the buckling of the sheet and affected the sheet load by less than 2 percent.

Normal pressure did not appreciably reduce the strain for buckling between rivets.

The combined effects of normal pressure and panel length caused a variation in average axial stress at failure from 19.9 ksi for a 19-inch panel with 8 psi of vacuum to 32.7 ksi for a 12-inch panel with  $-1/2$  psi of vacuum. Increasing sheet thickness from 0.025 to 0.051 inch caused a 7-percent reduction in average stress at failure, corresponding to the smaller reinforcement ratio.

The critical buckling strain of the sheet was found to depend on the sheet thickness, the lateral pressure, and the restraint of the sheet at the stringer edge. It was not affected by panel width, panel length, and direction of normal pressure (on sheet side or on stringer side). Analysis of the data indicated that the critical buckling strain for small lateral pressures depended principally on the flexural rigidity of the sheet and on the type of edge restraint; it was increased with an increase in sheet thickness and an increase in edge restraint. At large lateral pressures, on the other hand, the buckling strain depended principally on the amount of transverse curvature produced by the dishing under pressure; it was decreased with an increase in sheet thickness and an increase in edge restraint. As a result of the opposite effects of changes in sheet thickness at low pressure and at high pressure the measured buckling strains for the panels with 0.025-inch sheet exceeded those for the panels with 0.051-inch sheet for lateral pressures greater than 8 psi. Empirical formulas were derived to describe the effects on the buckling strain of changes in sheet thickness, lateral pressure, and edge restraint for panels similar to those tested.



The sheet load per bay was unaffected by the panel width, panel length, or direction of application of the normal load (i.e., pressure or vacuum). The sheet load for a given edge strain was decreased by lateral pressure for strains less than the buckling strain with no lateral pressure, but was increased for strains somewhat greater than the buckling strain with no lateral pressure. The measured load for all values of lateral pressure was greater than that given by Marguerre's formula for the effective width of a sheet with simply supported edges, without lateral pressure, except at loads below the buckling load with no lateral pressure.

Lateral pressure caused a small reduction (about 1/2 percent per psi) in the axial load at failure for the 12-inch panels and a somewhat greater reduction (about 2 percent per psi) for the 19-inch panels. The direction of the lateral pressure had no effect on the magnitude of this reduction. The panels with 0.025-inch sheet showed approximately the same reduction as the panels with 0.051-inch sheet.

The maximum axial load for all panels tested with 4 psi or less of normal pressure agreed within 6 percent with values obtained from a nomogram (reference 6) designed to predict the maximum axial load of panels without normal pressure. A simple correction formula to take account of the reduction in axial load at failure due to normal load is presented. The nomogram, together with this correction formula, gave maximum loads which agreed within 6 percent with the observed maximum loads for 27 of the 29 panels tested. The remaining two panels failed at loads 9 percent more and 18 percent less, respectively, than the predicted loads.

National Bureau of Standards,  
Washington, D. C., July 24, 1945.

## REFERENCES

1. Rafel, Norman, and Sandlin, Charles W.: Effect of Normal Pressure on the Critical Compressive and Shear Stress of Curved Sheet. NACA ARR No. L5B10 , March 1945.
2. Levy, Samuel, Goldenberg, Daniel, and Zibritosky, George: Simply Supported Long Rectangular Plate under Combined Axial Load and Normal Pressure. NACA TN No. 949, 1944.
3. Paul, D. A., Howell, F. M., and Grieshaber, H. E.: Comparison of Stress-Strain Curves Obtained by Single-Thickness and Pack Methods. NACA TN No. 819, 1941.
4. Ramberg, Walter, McPherson, Albert E., and Levy, Sam.: Compressive Tests of a Monocoque Box. NACA TN No. 721, 1939.
5. Timoshenko, S.: Theory of Plates and Shells. McGraw-Hill Book Co., Inc., 1940. p. 206.
6. Levy, Samuel, McPherson, Albert E., and Ramberg, Walter: Effect of Rivet and Spot-Weld Spacing on the Strength of Axially Loaded Sheet-Stringer Panels of 24S-T Aluminum Alloy. NACA TN No. 856, 1942.
7. Timoshenko, S.: Strength of Materials. Vol. 2., D. Van Nostrand Co., Inc., 1930.

TABLE 1.- DIMENSIONS OF PANELS AND MAXIMUM NORMAL PRESSURE

[See also fig. 1.]

Panel number	Normal <sup>1</sup> pressure, p (psi)	Length of panel, l (in.)	Thickness of sheet, t (in.)	Width of panel, W (in.)	Cross-sectional area of panel (sq in.)	Cross-sectional area of stringer (sq in.)	Stringer spacing, b (in.)	Normal pressure ratio, $\frac{pb^4}{Et^4}$
1	-8	11.92	0.0251	16.73	1.306	0.178	4.00	495
2	-4	11.98	.0252	16.75	1.300	.176	4.00	237
3	-2	11.96	.0251	16.70	1.400	.196	4.00	123
4	-1	11.92	.0249	16.73	1.369	.190	4.00	63.4
5	-1/2	11.97	.0253	16.75	1.359	.187	4.00	29.2
6	0	11.98	.0249	16.75	1.365	.189	4.00	0
7	4	11.98	.0250	16.75	1.272	.171	4.00	250
8	8	11.96	.0250	16.75	1.303	.177	4.00	512
9	12	11.97	.0250	16.75	1.290	.174	4.00	735
10	16	11.98	.0250	16.75	1.302	.177	4.00	979
11	-8	11.93	.0513	16.75	1.770	.182	4.00	27.4
12	-2	11.96	.0515	16.75	1.744	.176	4.00	6.74
13	-1/2	11.96	.0507	16.73	1.733	.177	4.00	1.83
14	0	11.96	.0511	16.75	1.738	.176	4.00	0
15	4	11.97	.0516	16.75	1.743	.176	4.00	13.2
16	8	11.95	.0515	16.75	1.773	.182	4.00	27.0
17	16	11.96	.0520	16.75	1.741	.174	4.00	51.9
18	-8	18.96	.0250	16.76	1.258	.168	4.00	499
19	-1/2	18.92	.0254	16.75	1.419	.199	4.00	31.2
20	0	18.94	.0256	16.75	1.376	.191	4.00	0
21	8	18.93	.0257	16.78	1.391	.192	4.00	447
22	-8	18.94	.0517	16.72	1.757	.179	4.00	27.0
23	-2	18.95	.0523	16.75	1.778	.180	4.00	6.46
24	0	18.94	.0516	16.75	1.818	.191	4.00	0
25	8	18.94	.0521	16.75	1.758	.177	4.00	26.2
26	-8	18.94	.0259	24.76	2.048	.201	4.00	425
27	-1	18.94	.0262	24.76	1.898	.179	4.00	51.7
28	0	18.93	.0259	24.76	2.036	.200	4.00	0
29	8	18.90	.0258	24.77	1.874	.177	4.00	432

<sup>1</sup>Positive values indicate pressure on sheet side; negative values indicate vacuum on sheet side.

TABLE 2.- TENSILE AND COMPRESSIVE PROPERTIES OF SHEET

[See also fig. 2.]

NACA TN No. 1041.

Sheet used in panels <sup>1</sup>	Direction of rolling	Young's modulus		Yield strength (offset=0.2%)		Secant <sup>2</sup> yield strength compression (ksi)	Tensile strength (ksi)
		Tension (ksi)	Compression (ksi)	Tension (ksi)	Compression (ksi)		
A	Longitudinal	10,100	10,500	56.5	47.0	47.3	70.7
	Transverse	10,300	-	48.9	-	-	68.6
B	Longitudinal	10,500	10,700	52.6	46.0	45.2	72.2
	Transverse	10,300	-	46.7	-	-	69.7
C	Longitudinal	10,300	10,800	58.6	48.4	48.1	72.9
	Transverse	10,300	-	50.1	-	-	71.6
D	Longitudinal	10,300	10,600	58.6	48.7	48.6	73.5
	Transverse	10,300	-	50.0	-	-	72.2

<sup>1</sup>A, panels 1, 3, 4, 7, 8, 18, 19, 20, 21, 27

B, panels 2, 5, 6, 9, 10, 26, 28, 29

C, panels 11, 12, 14, 15, 16, 17

D, panels 13, 22, 23, 24, 25

<sup>2</sup>Stress at intercept of stress-strain curve and secant line through origin with slope 0.7E.

TABLE 3.-- STRAINS AT FIRST OBSERVED BUCKLING OF SHEET

Panel	Buckling of sheet between stringers		Buckling of sheet between rivets
	Part way between stringers	Stringer to stringer	
1	0.0031	0.00125	(1)
2	(1)	.00094	(1)
3	.00058	.00061	(1)
4	(1)	.00055	(1)
5	(1)	.00041	(1)
6	(1)	.00040	(1)
7	(1)	.00130	(1)
8	.00151	.00155	<sup>2F</sup>
9	.0025	.0018	(1)
10	.0030	.0027	<sup>2F</sup>
11	(1)	.00158	<sup>2F</sup>
12	(1)	.00105	<sup>2F</sup>
13	(1)	.00089	(1)
14	(1)	.00090	(1)
15	(1)	.0011	(1)
16	(1)	.0013	<sup>2F</sup>
17	(1)	.0022	<sup>2F</sup>
18	(1)	.0009	(1)
19	(1)	.00044	(1)
20	(1)	.00046	(1)
21	(1)	.0016	(1)
22	(1)	.00087	(1)
23	(1)	.00089	(1)
24	(1)	.00087	<sup>2F</sup>
25	(1)	.0018	<sup>2F</sup>
26	(1)	.0012	(1)
27	(1)	.0007	(1)
28	(1)	.00055	(1)
29	(1)	.0017	(1)

<sup>1</sup>None observed.<sup>2F</sup>, observed either at or just prior to failure.

TABLE 4.- FAILURE OF PANELS

Panel	Sheet thickness (in.)	Pressure <sup>1</sup> on sheet side (psi)	Panel length (in.)	Maximum axial load, P (kips)	Average axial stress, P/A (ksi)
1	0.0251	-8	11.92	39.2	30.0
2	.0252	-4	11.98	40.8	31.4
3	.0251	-2	11.96	45.5	32.5
4	.0249	-1	11.92	44.4	32.5
5	.0253	-1/2	11.97	44.4	32.7
6	.0249	0	11.98	43.6	32.0
7	.0250	4	11.98	39.2	30.8
8	.0250	8	11.96	39.9	30.6
9	.0250	12	11.97	39.3	30.5
10	.0250	16	11.98	38.5	29.6
11	.0513	-8	11.93	51.6	29.2
12	.0515	-2	11.96	52.1	29.9
13	.0507	-1/2	11.96	51.7	29.8
14	.0511	0	11.96	51.3	29.5
15	.0516	4	11.97	49.9	28.6
16	.0515	8	11.95	49.8	28.1
17	.0520	16	11.96	47.0	27.0
18	.0250	-8	18.96	25.0	19.9
19	.0254	-1/2	18.92	43.5	30.7
20	.0256	0	18.94	41.3	30.0
21	.0257	8	18.93	37.0	26.6
22	.0517	-8	18.94	40.7	23.2
23	.0523	-2	18.95	49.4	27.8
24	.0516	0	18.94	52.4	28.8
25	.0521	8	18.94	40.5	23.0
26	.0259	-8	18.94	47.6	23.2
27	.0262	-1	18.94	53.2	28.0
28	.0259	0	18.93	59.5	29.2
29	.0258	8	18.90	46.6	24.8

<sup>1</sup>Negative values correspond to vacuum on sheet side.

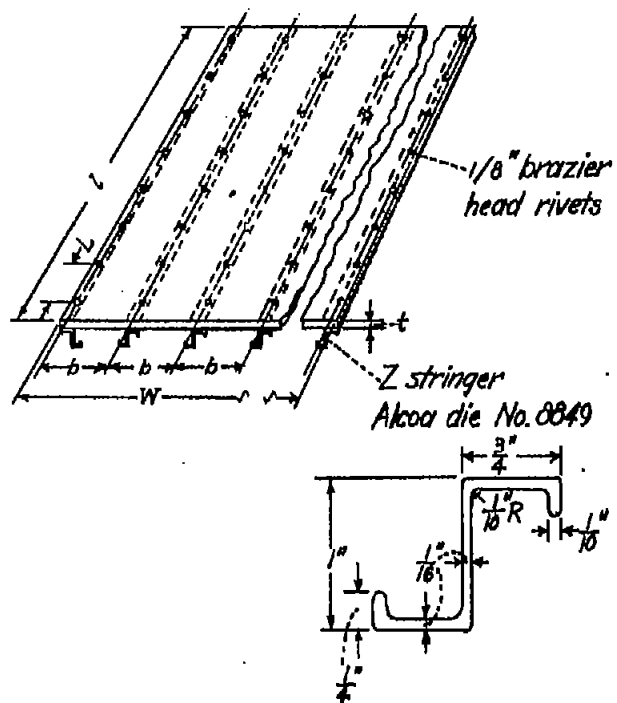


Figure 1.- Construction of sheet-stringer panels and nominal dimensions of stringer.

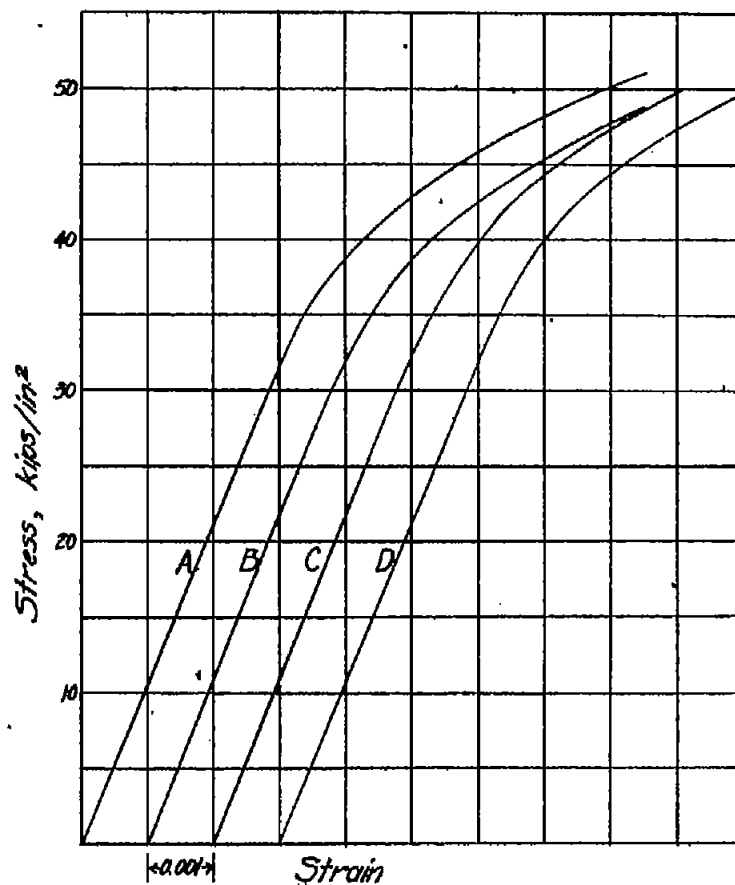


Figure 2.- Compressive stress-strain curves of sheet material: A, panels 1,3,4,7,8,18,19,20,21,27; B, panels 2,5,6,9,10,26,28,29; C, panels 11,12,14,15,16,17; D, panels 13,22,23,24,25.

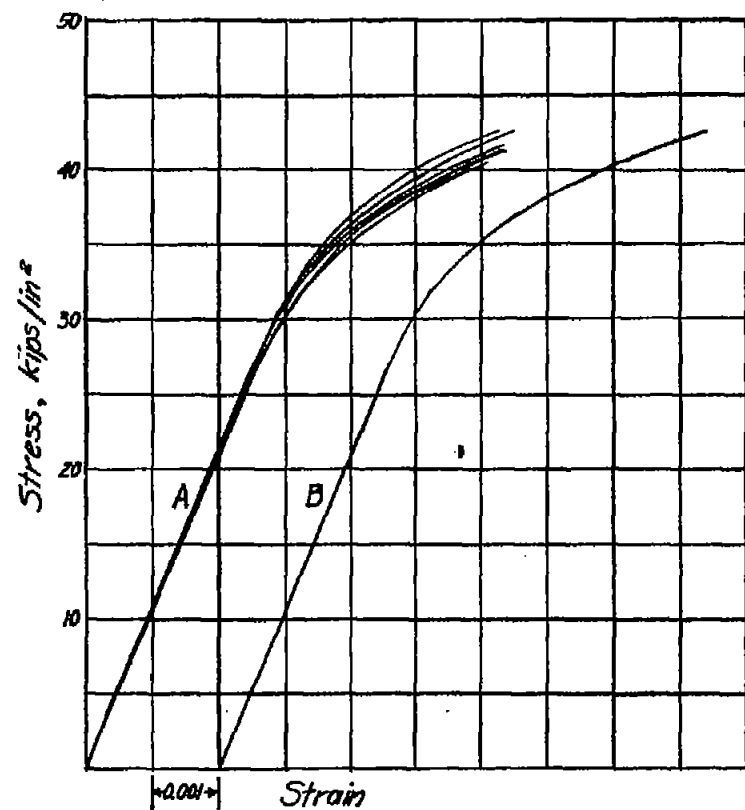


Figure 3.- Compressive stress-strain curves of four-inch lengths of 2-stringers; A, family of stress-strain curves for stringers of all panels; B, stress-strain curve used in computations for all panels.

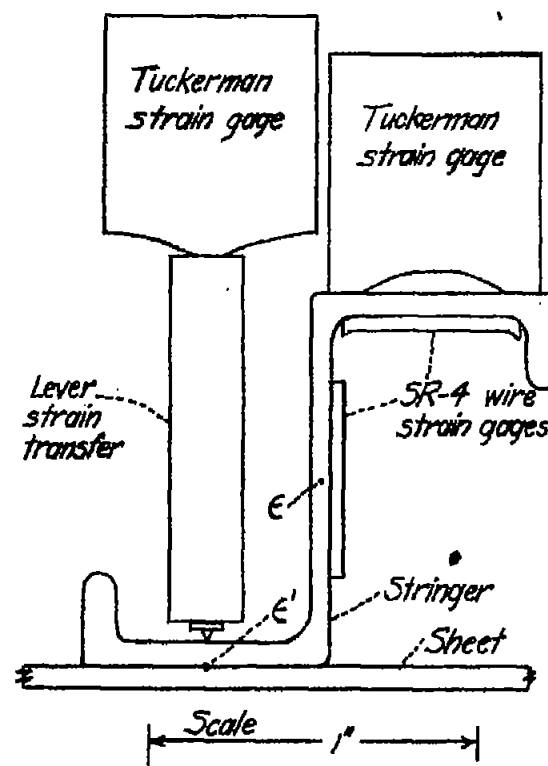


Figure 7.- Location of strain gages on stringer cross-section.



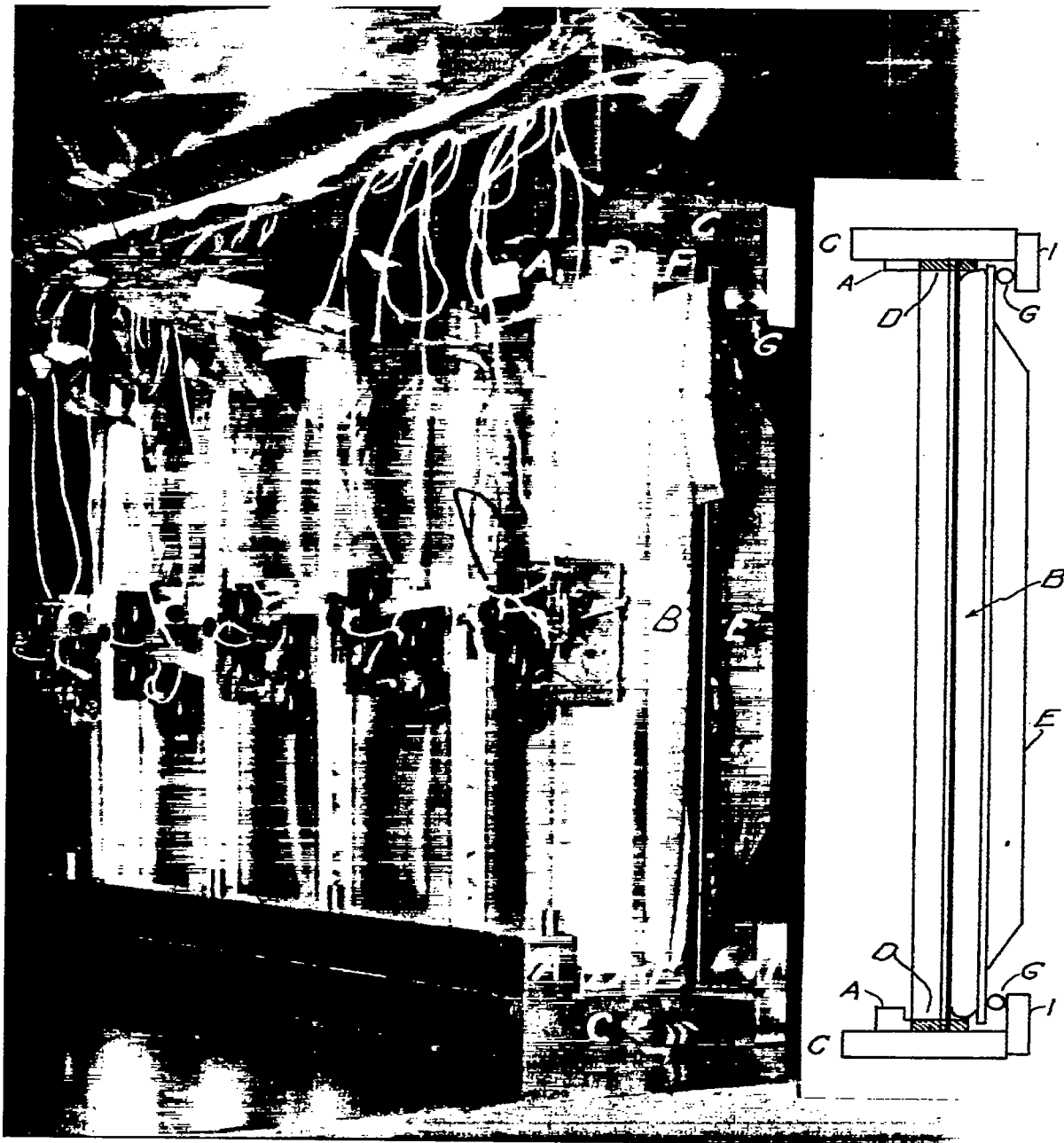


Figure 4.- Panel with pressure on sheet side, showing panel side of jig.

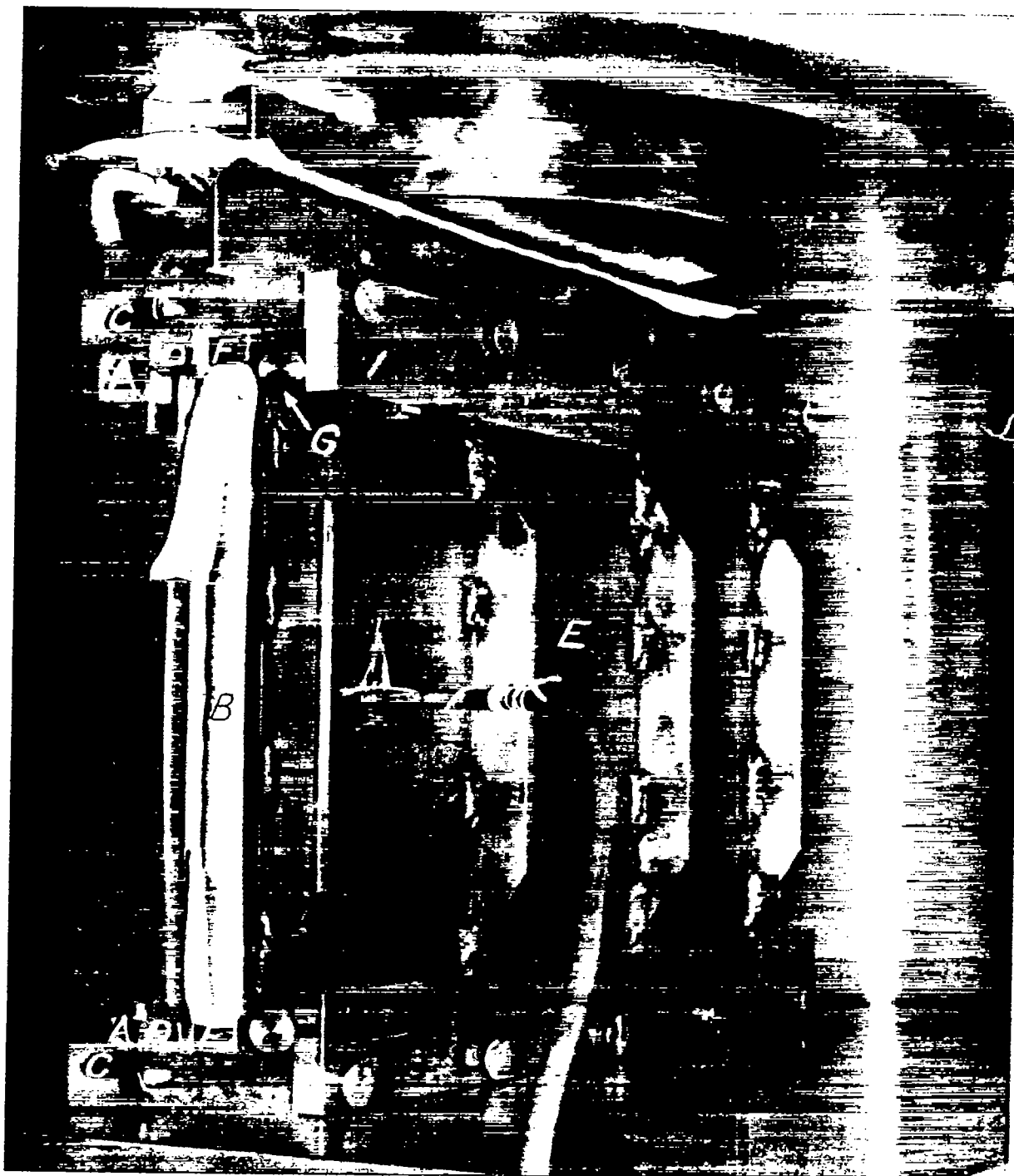


Figure 5.- Panel with pressure on sheet side, showing back of jig.

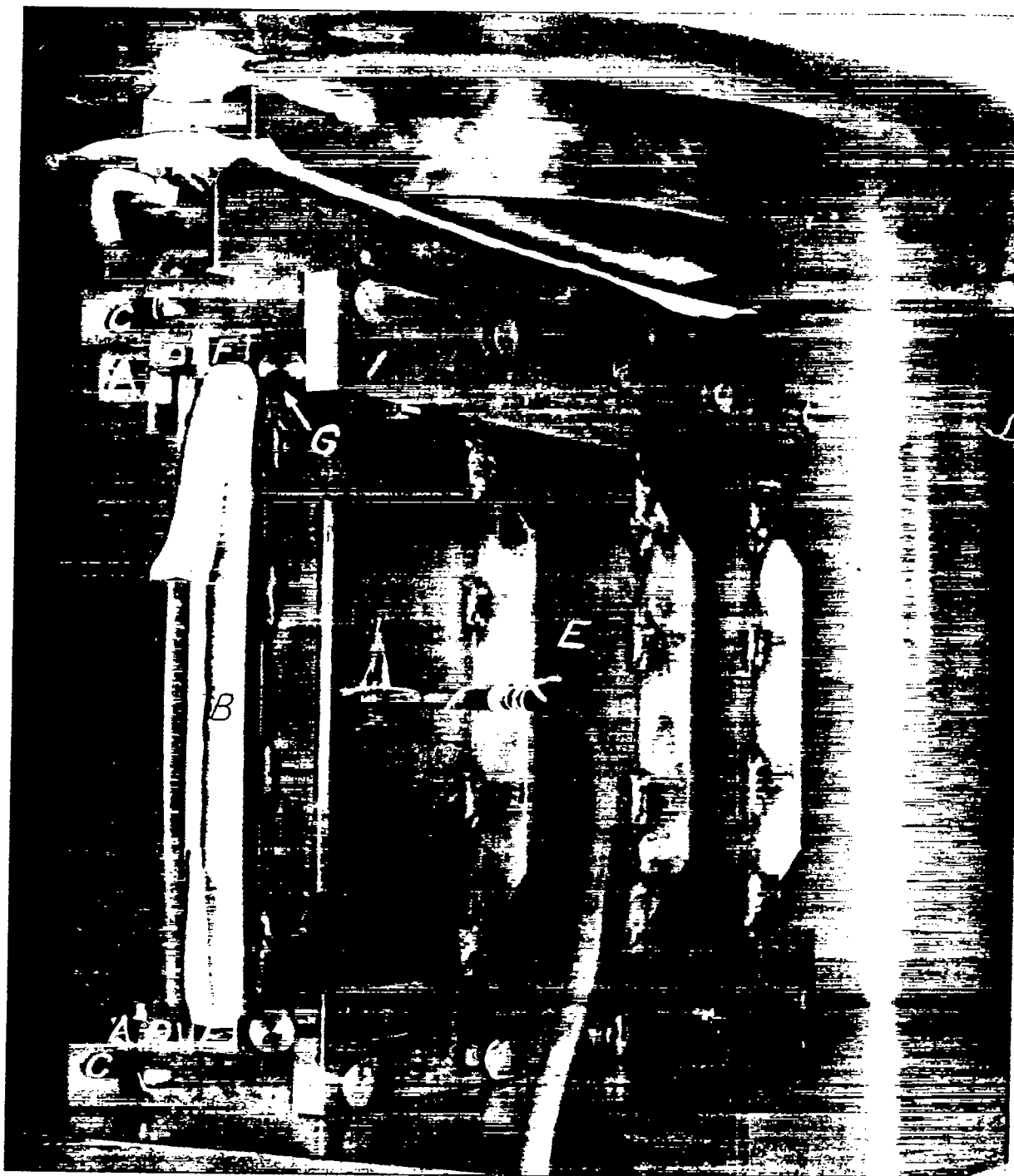


Figure 5.- Panel with pressure on sheet side, showing back of jig.

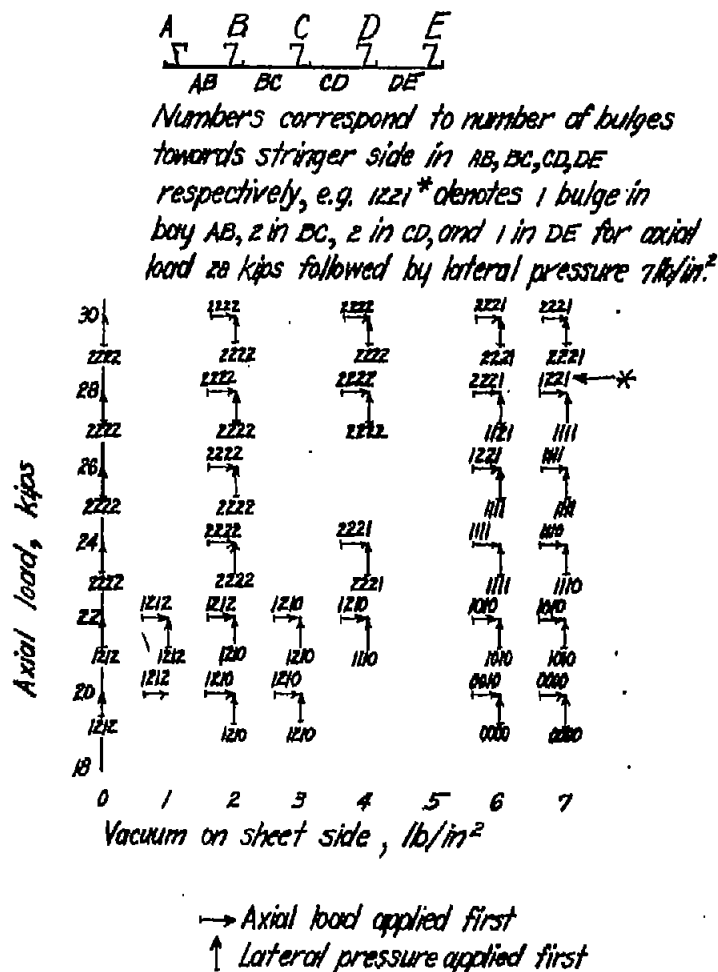


Figure 8.- Buckle pattern for panel 13 in the elastic range with vacuum on the sheet side from zero to 7 psi and axial load from 20 to 30 kips.

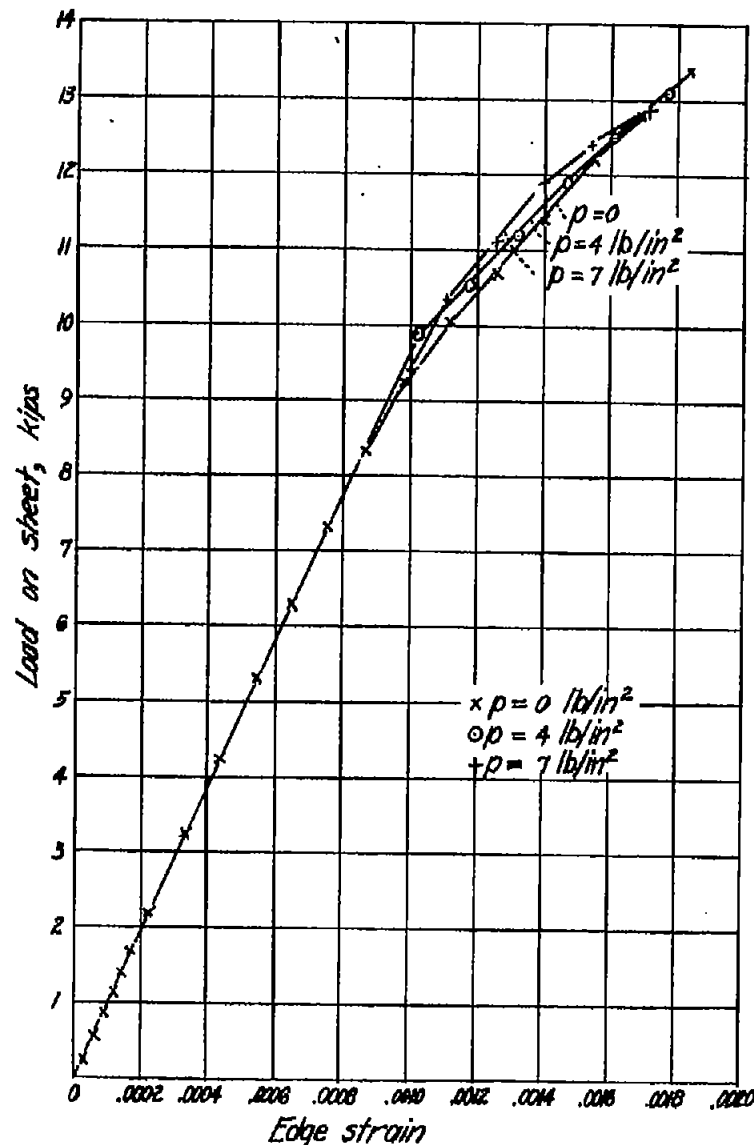


Figure 9.- Sheet load in the elastic range for panel 13 as a function of lateral pressure  $p$  and edge strain.

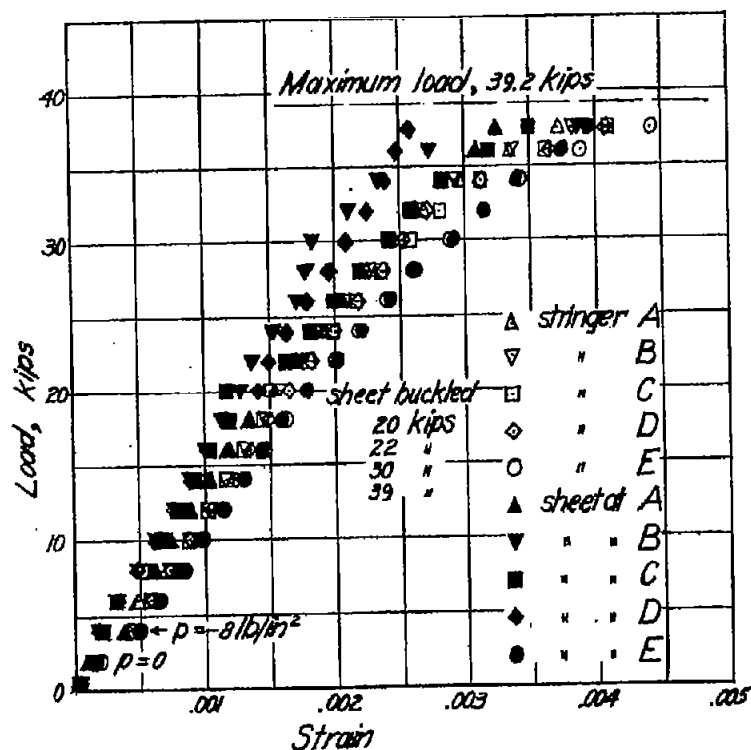


Figure 10.- Test of panel 1. Vacuum on sheet side, 8 psi; length, 12 inches; sheet thickness, 0.0251 in.

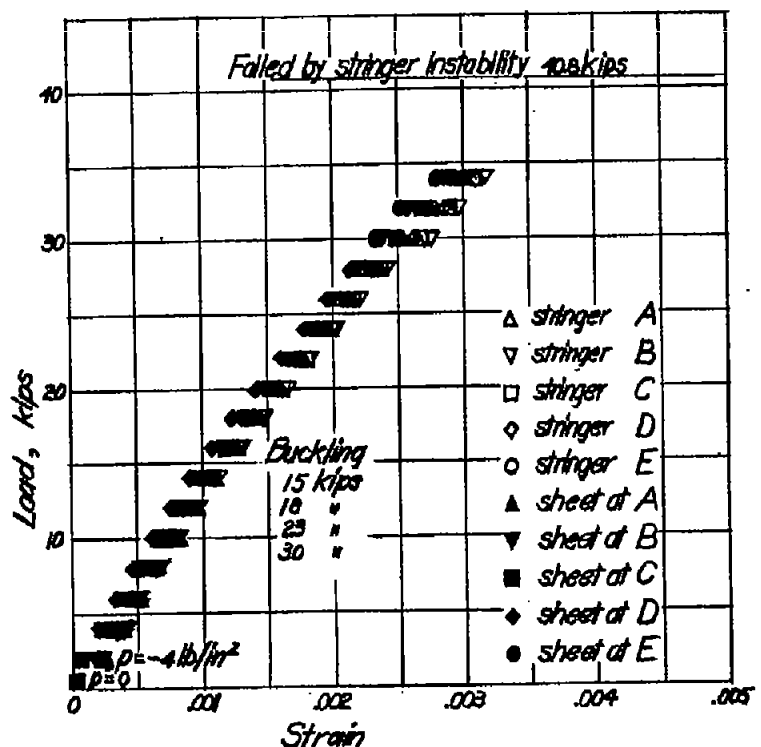


Figure 11.- Test of panel 2. Vacuum on sheet side, 4 psi; length, 12 inches; sheet thickness, 0.0252 in.

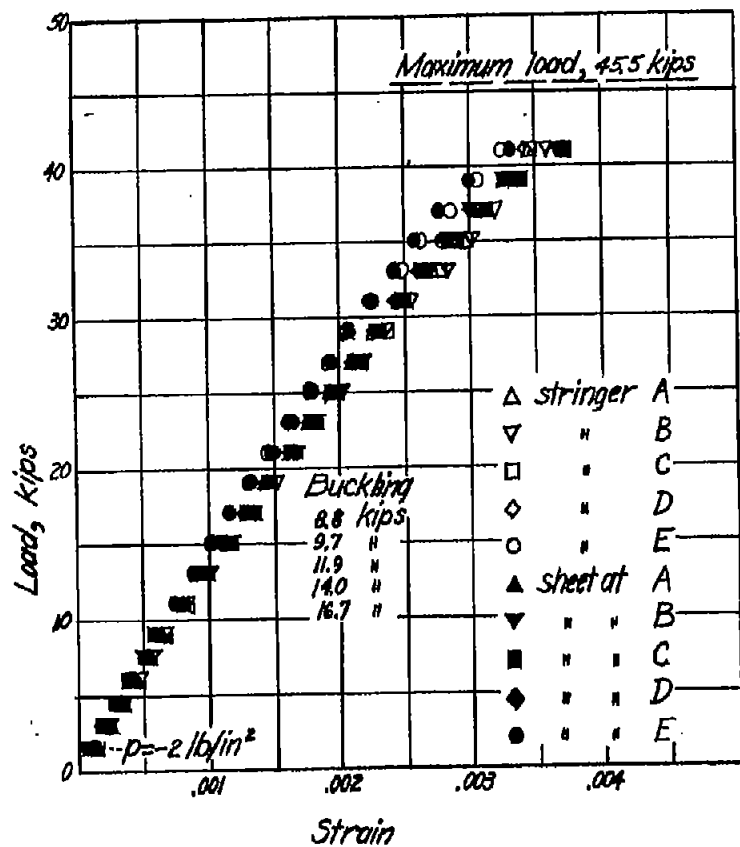


Figure 12.- Test of panel 3. Vacuum on sheet side, 3 psi; length, 12 inches; sheet thickness, 0.0261 in.

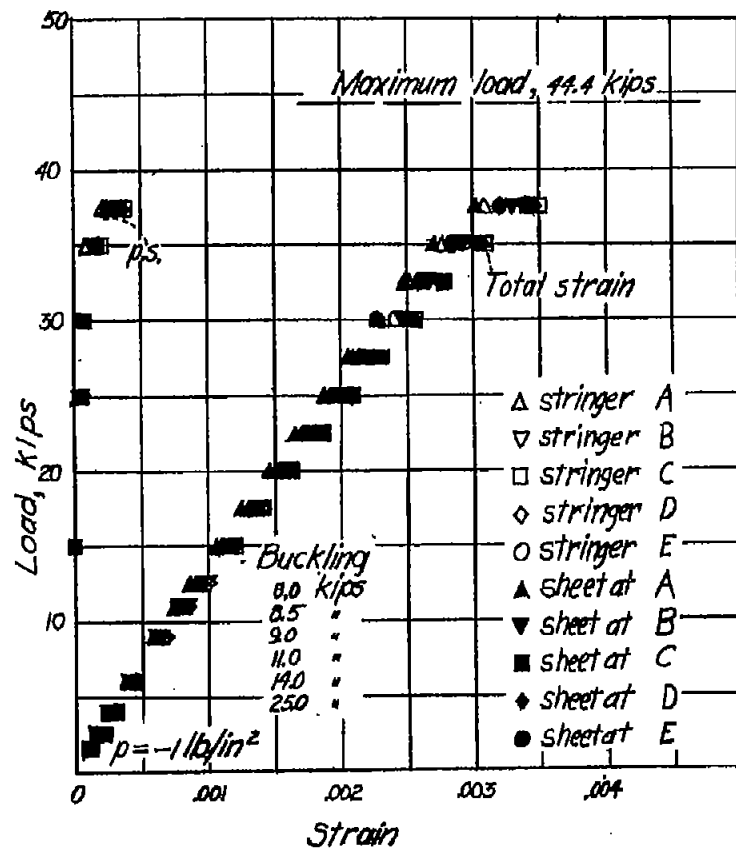


Figure 13.- Test of panel 4. Vacuum on sheet side, 1 psi; length, 12 inches; sheet thickness, 0.0249 in.

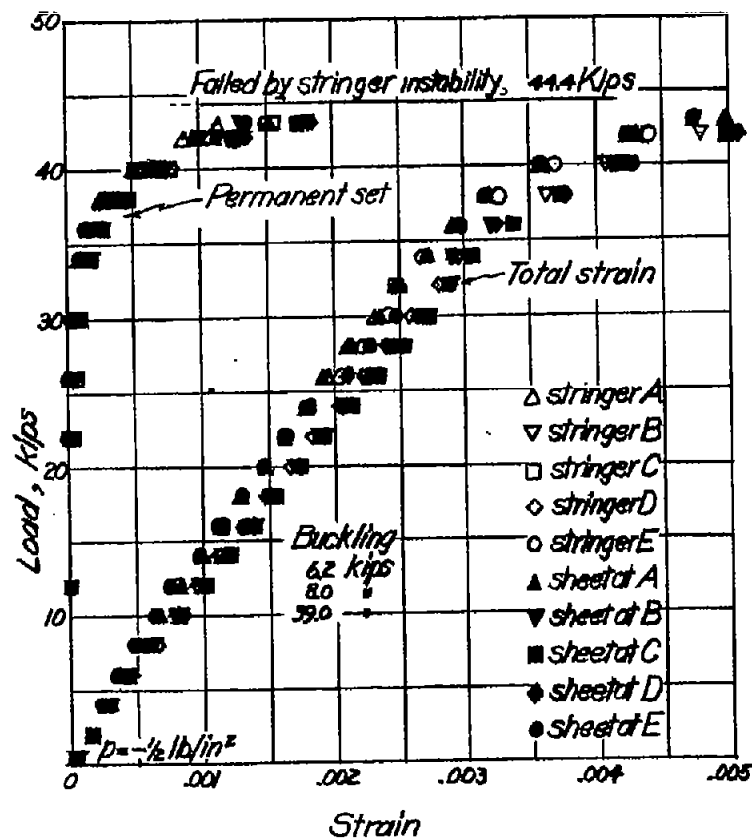


Figure 14.- Test of panel 5. Vacuum on sheet side, 1/2 psi; length, 18 inches; sheet thickness, 0.0253 in.

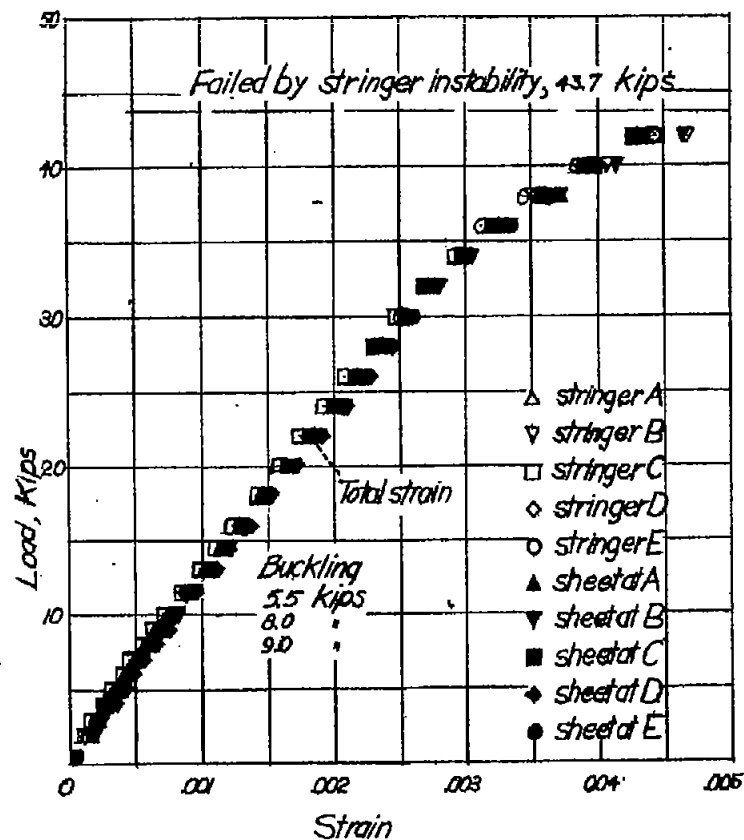


Figure 15.- Test of panel 6. No lateral pressure; length, 12 inches; sheet thickness, 0.0249 in.

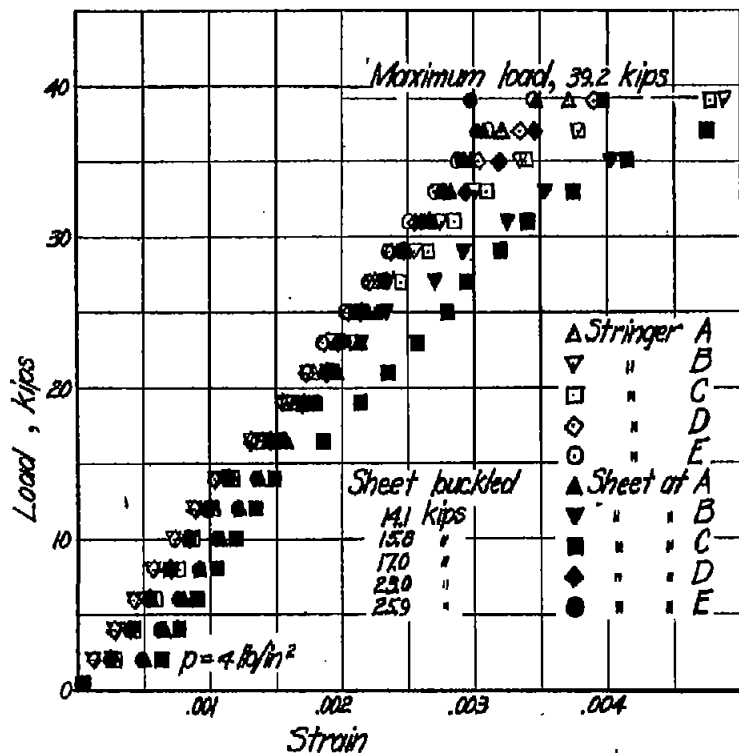


Figure 16.- Test of panel 7. Pressure on sheet side, 4 psi; length, 12 inches; sheet thickness, 0.0250 in.

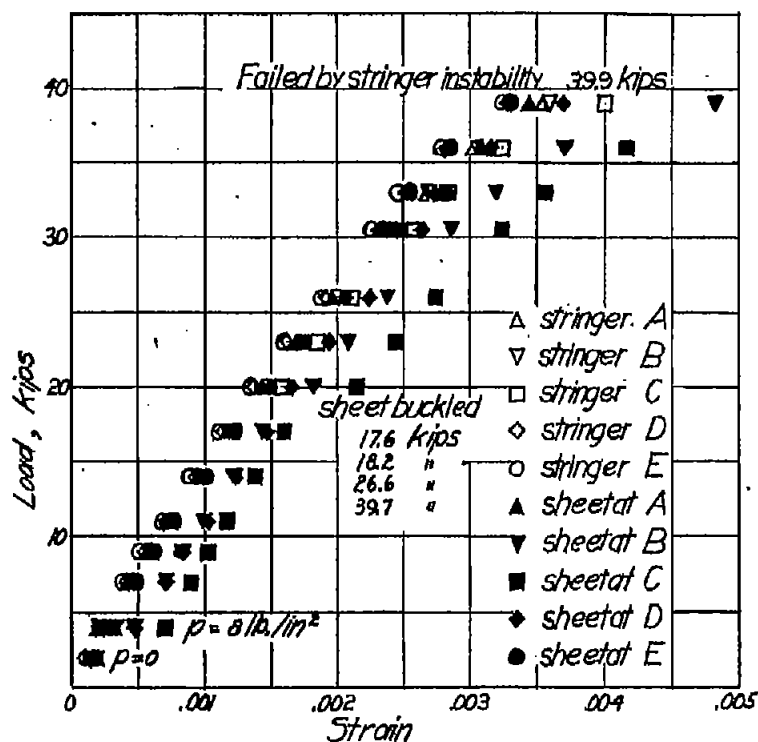


Figure 17.- Test of panel 8. Pressure on sheet side, 8 psi; length, 12 inches; sheet thickness, 0.0250 in.



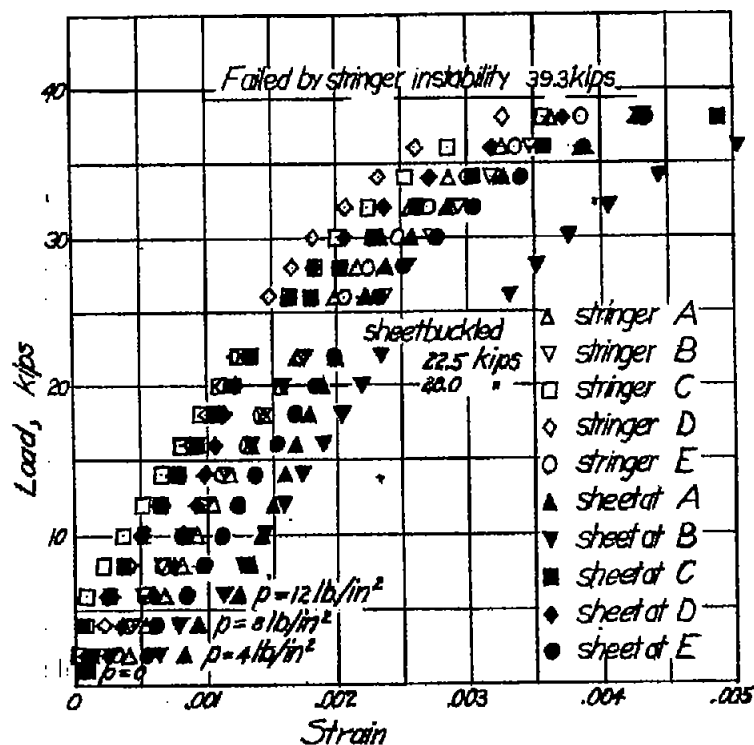


Figure 18.- Test of panel 9. Pressure on sheet side, 12 psi; length, 12 inches; sheet thickness, 0.0250 in.

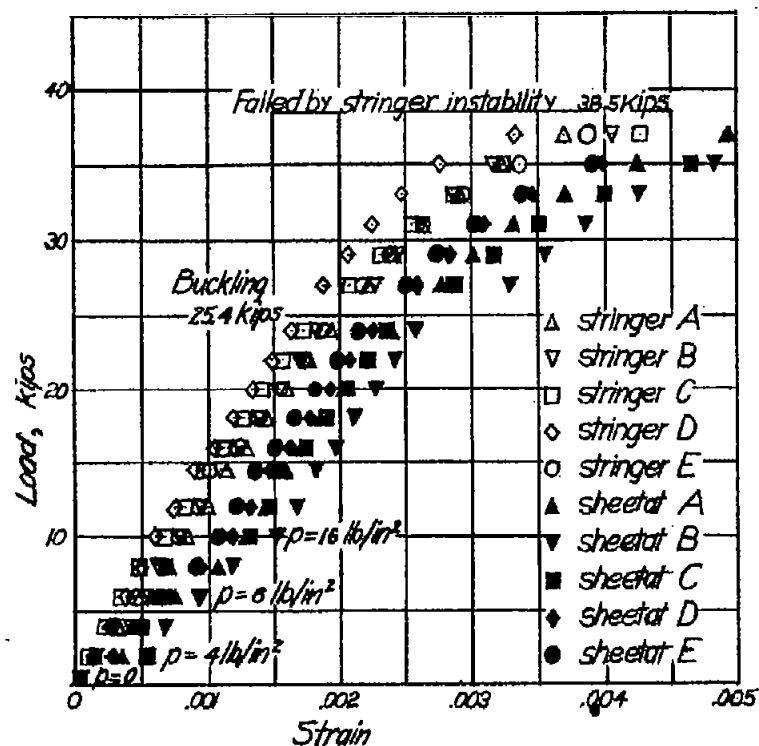


Figure 19.- Test of panel 10. Pressure on sheet side, 16 psi; length, 12 inches; sheet thickness, 0.0250 in.

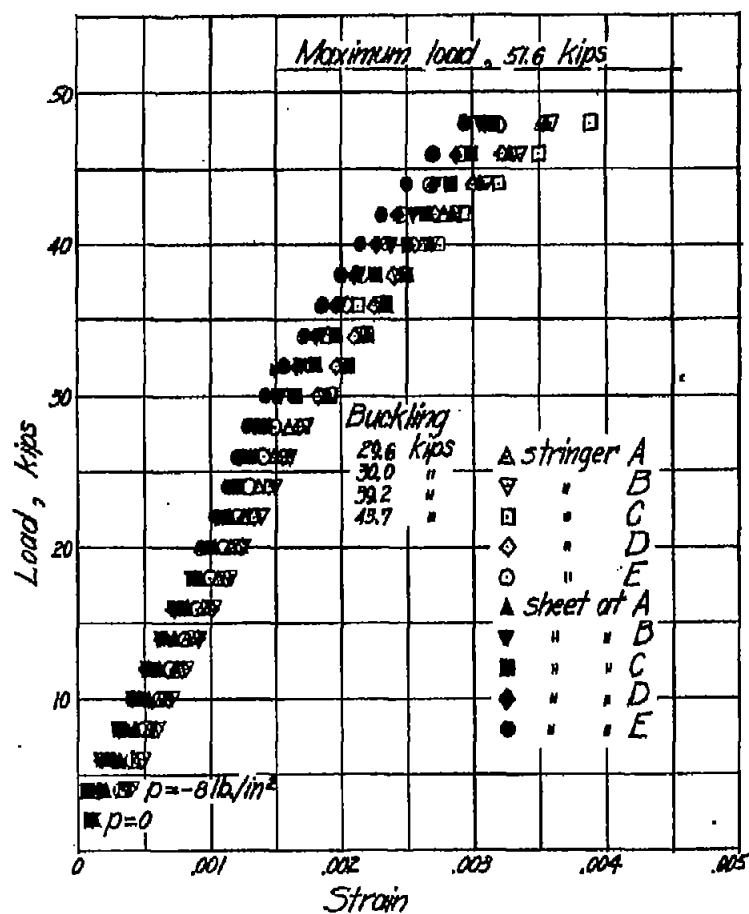


Figure 30.- Test of panel 11. Vacuum on sheet side, 8 psi; length, 12 inches; sheet thickness, 0.0613 in.

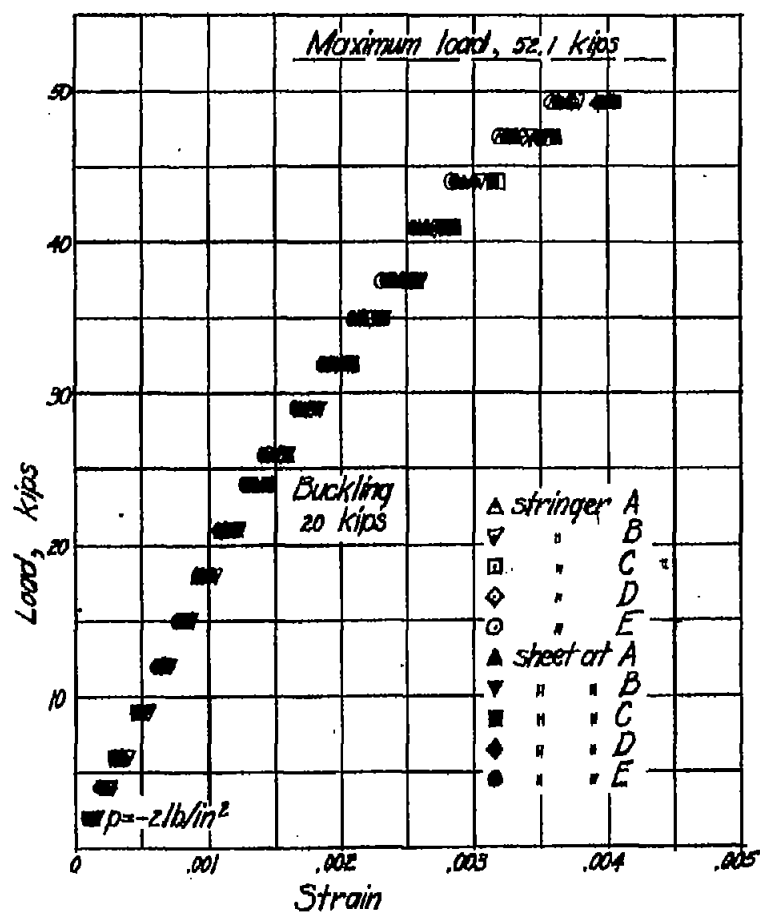


Figure 31.- Test of panel 12. Vacuum on sheet side, 2 psi; length, 12 inches; sheet thickness, 0.0615 in.

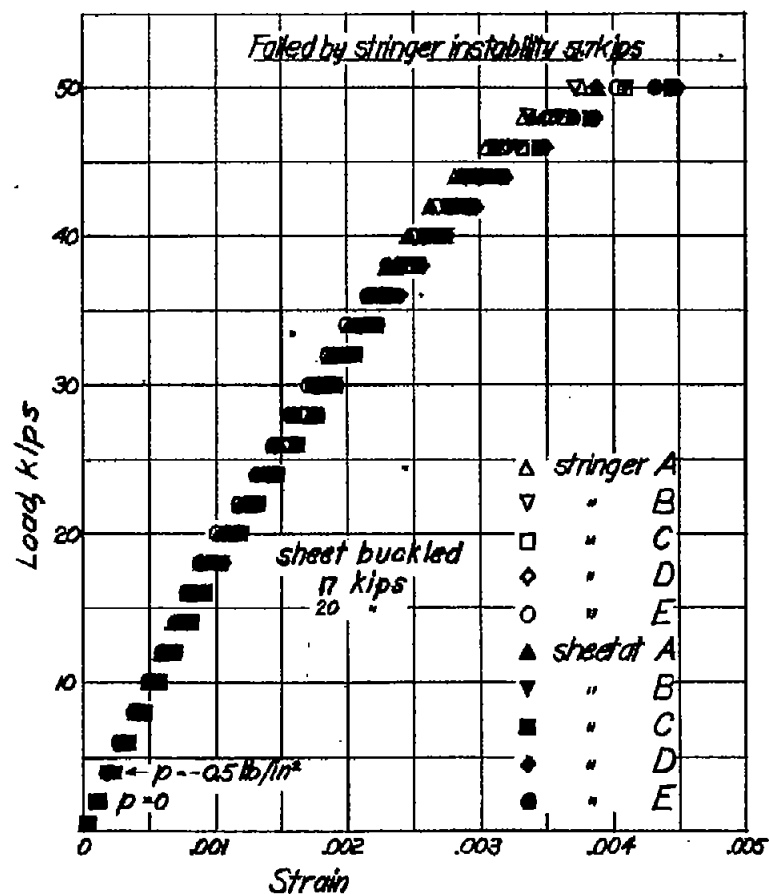


Figure 22.- Test of panel 13. Vacuum on sheet side, 1/2 psi; length, 11.96 inches; sheet thickness, 0.0507 in.

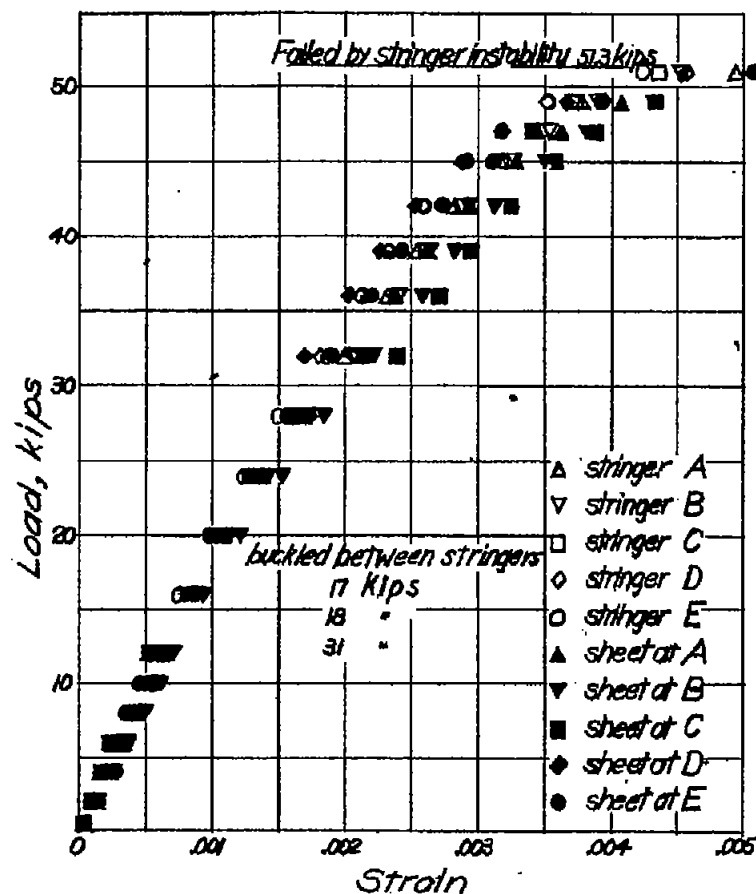


Figure 23.- Test of panel 14. Zero lateral pressure; length, 12 inches; sheet thickness, 0.0511 in.

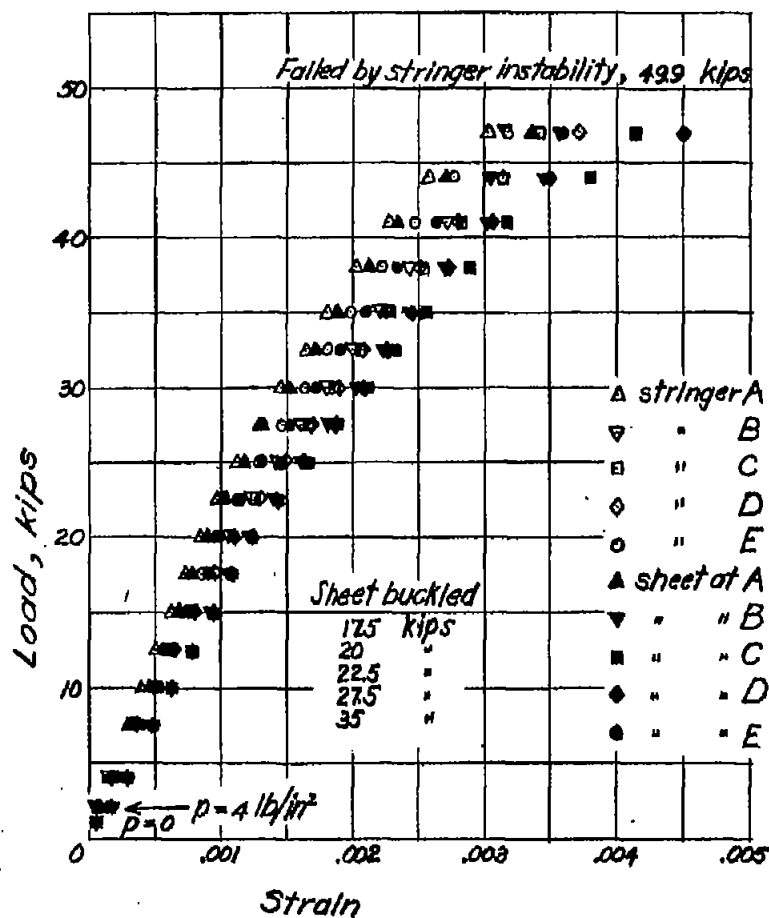


Figure 24.- Test of panel 15. Pressure on sheet side, 4 psi; length, 12 inches; sheet thickness, 0.0516 in.

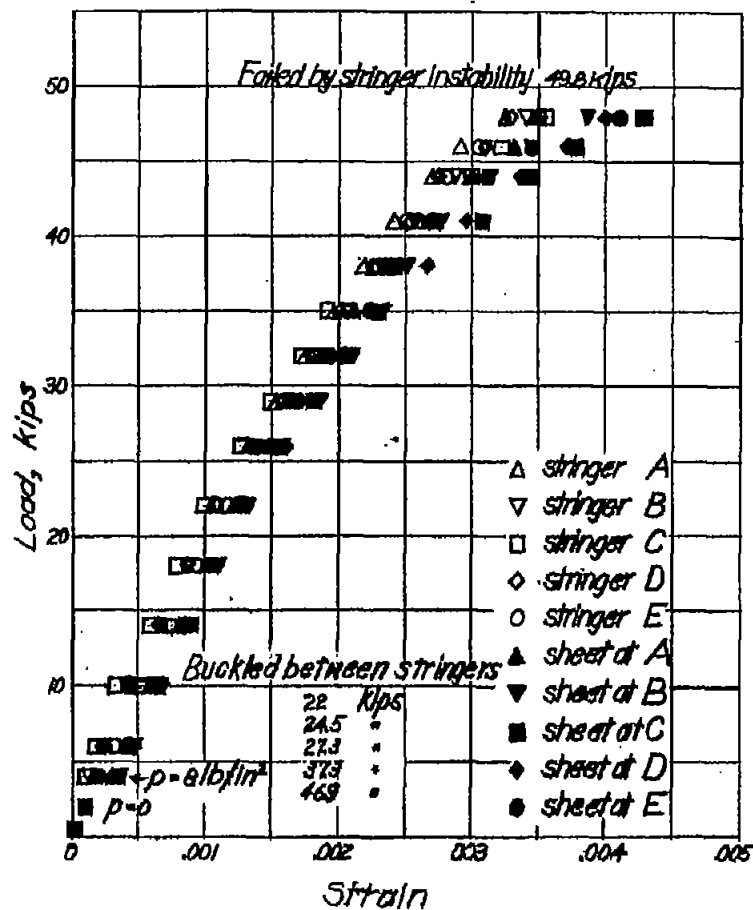


Figure 25.- Test of panel 16. Pressure on sheet side, 8 psi; length, 12 inches; sheet thickness, 0.0515 in.

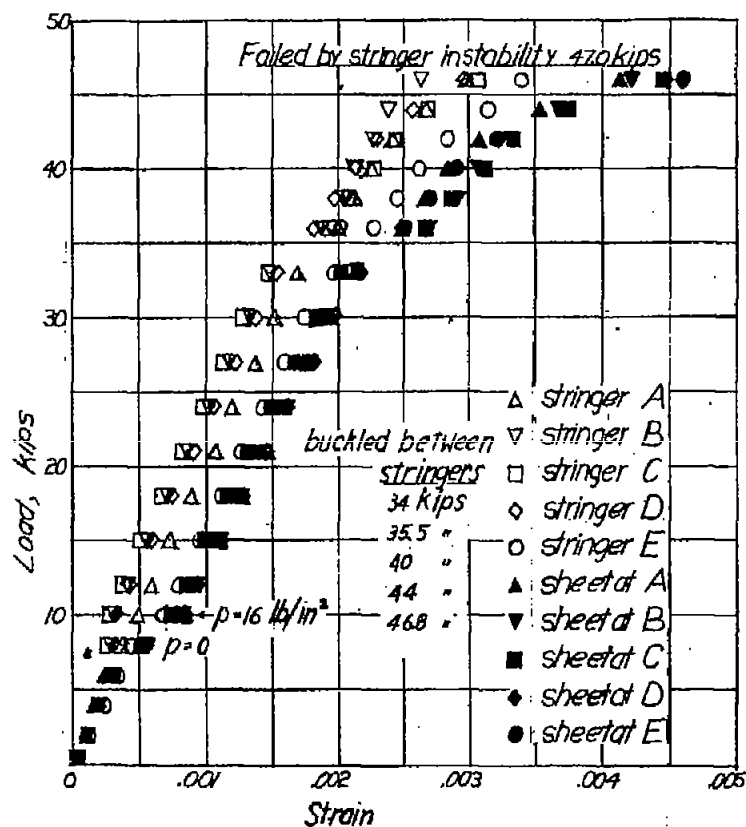


Figure 26.- Test of panel 17. Pressure on sheet side, 16 psi; length, 12 inches; sheet thickness, 0.0530 in.

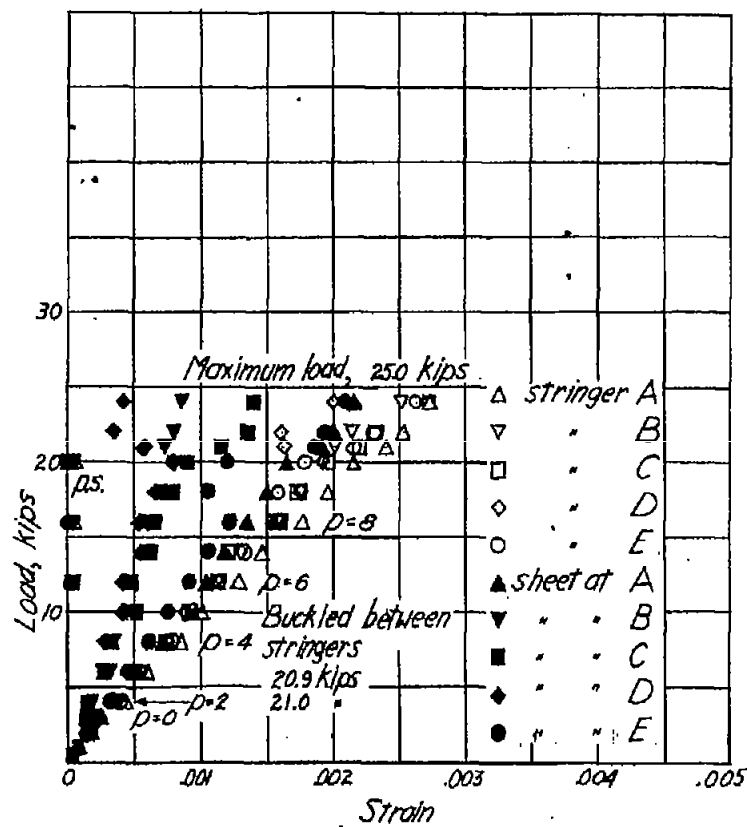


Figure 27.- Test of panel 18. Pressure on sheet side, 8 psi; length, 19 inches; sheet thickness, 0.0350 in.

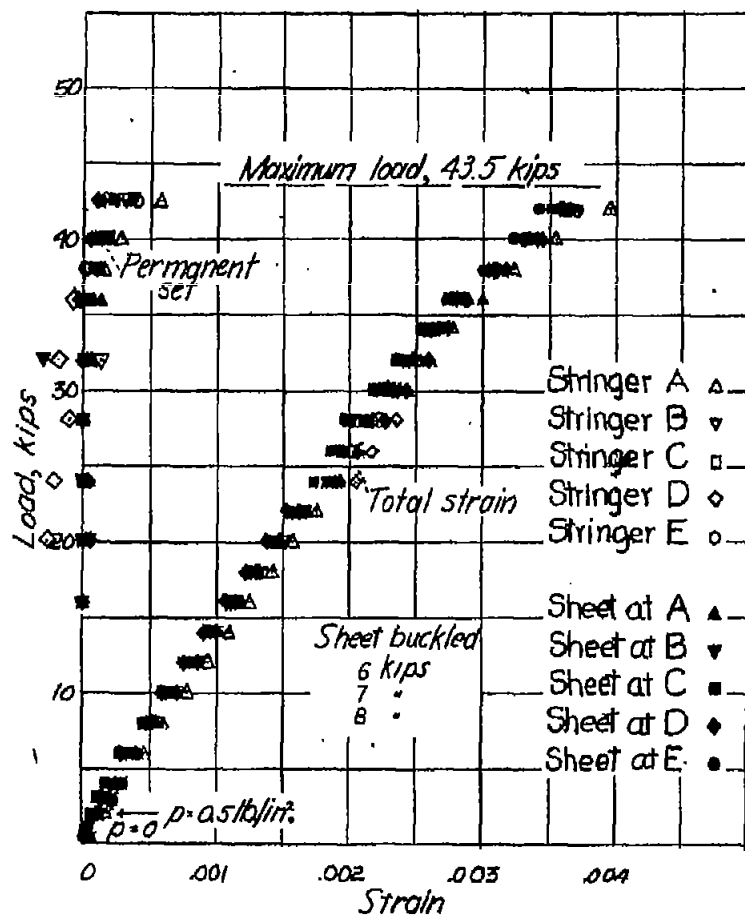


Figure 28.- Test of panel 19. Vacuum on sheet side, 0.5 psi; length, 19 inches; sheet thickness, 0.0254 in.

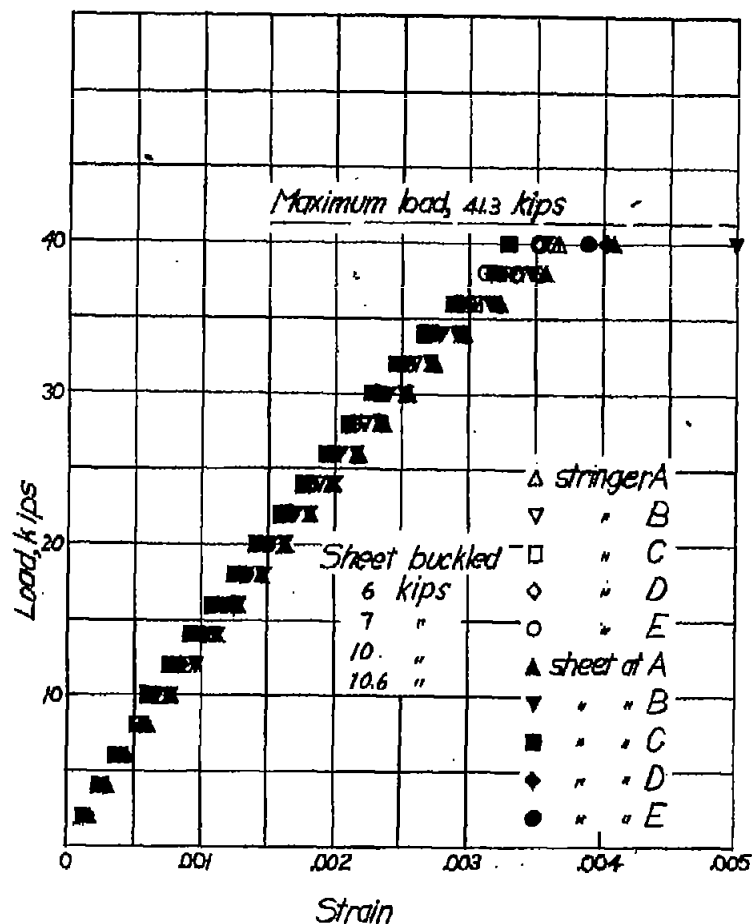


Figure 29.- Test of panel 20. No lateral pressure; length, 19 inches; sheet thickness, 0.0258 in.

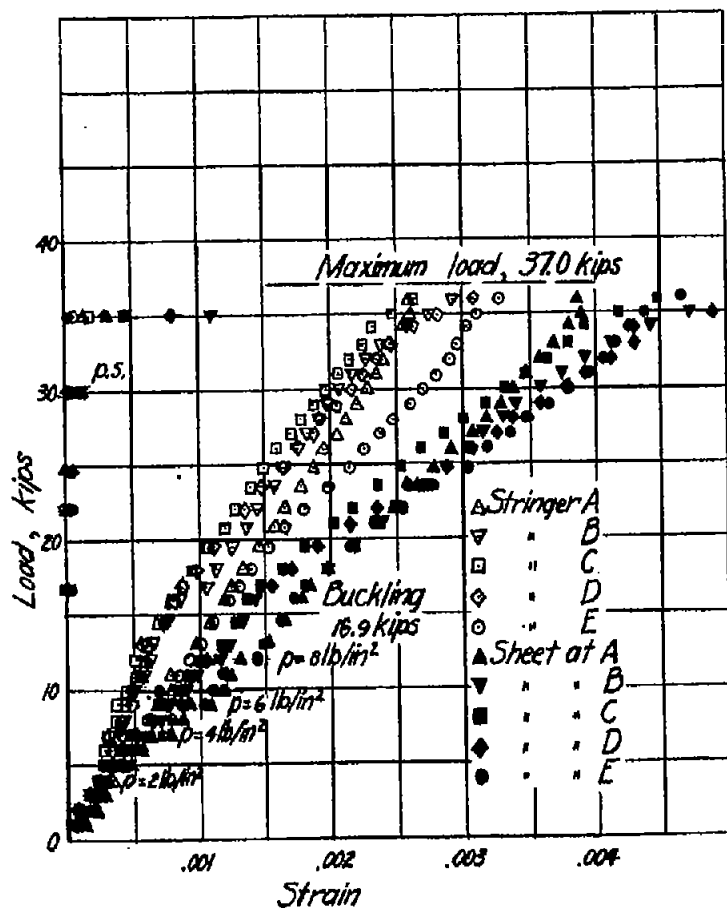


Figure 30.- Test of panel 21. Pressure on sheet side, 8 psi; length, 19 inches; sheet thickness, 0.0257 in.

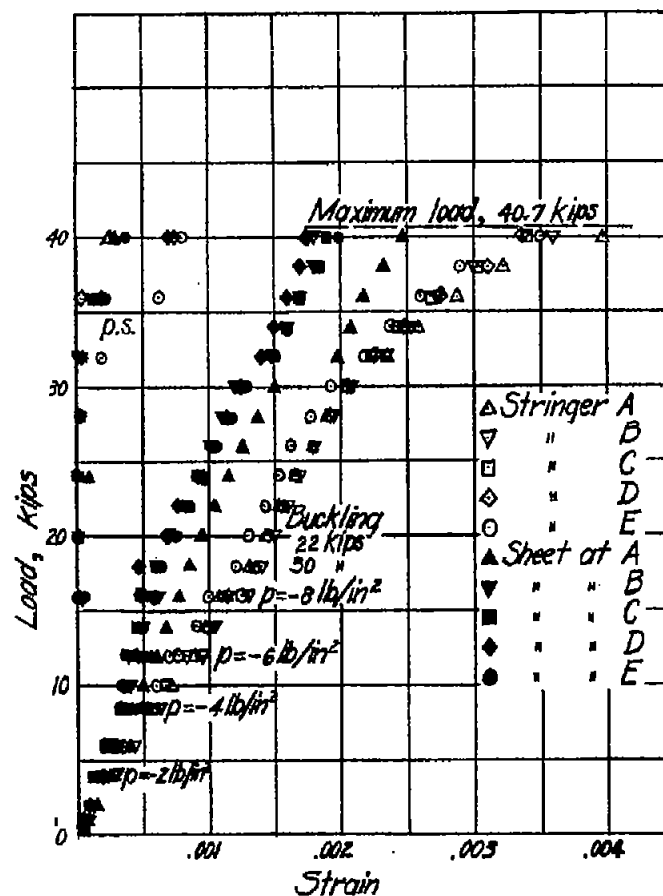


Figure 31.- Test of panel 23. Vacuum on sheet side, 8 psi; length, 19 inches; sheet thickness, 0.0517 in.

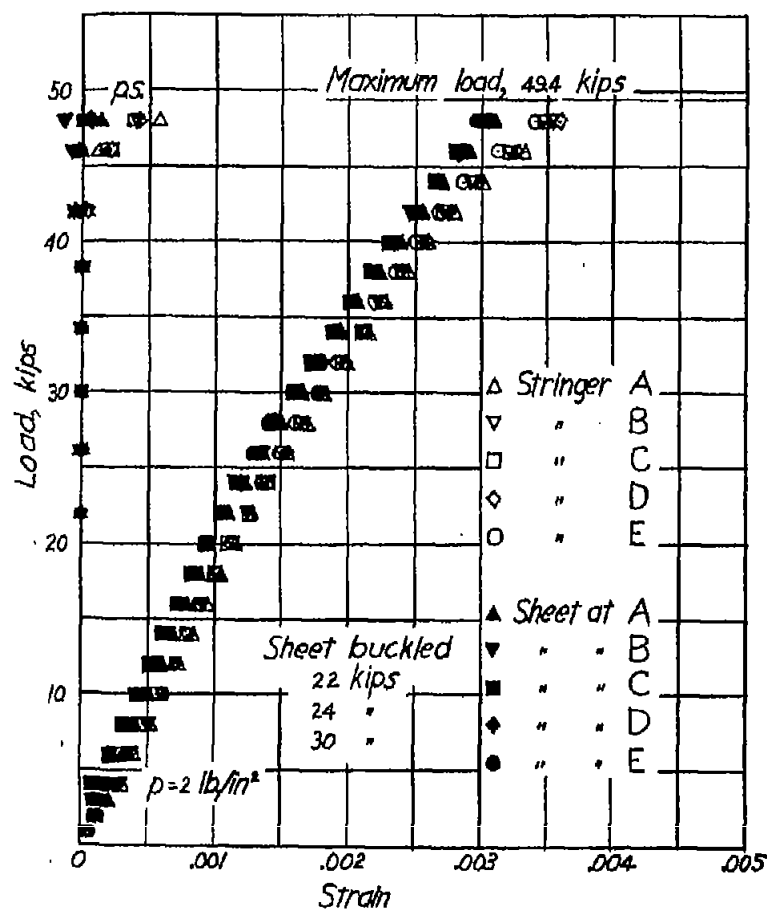


Figure 32.- Test of panel 23. Vacuum on sheet side, 2 psi; length, 19 inches; sheet thickness, 0.0523 in.

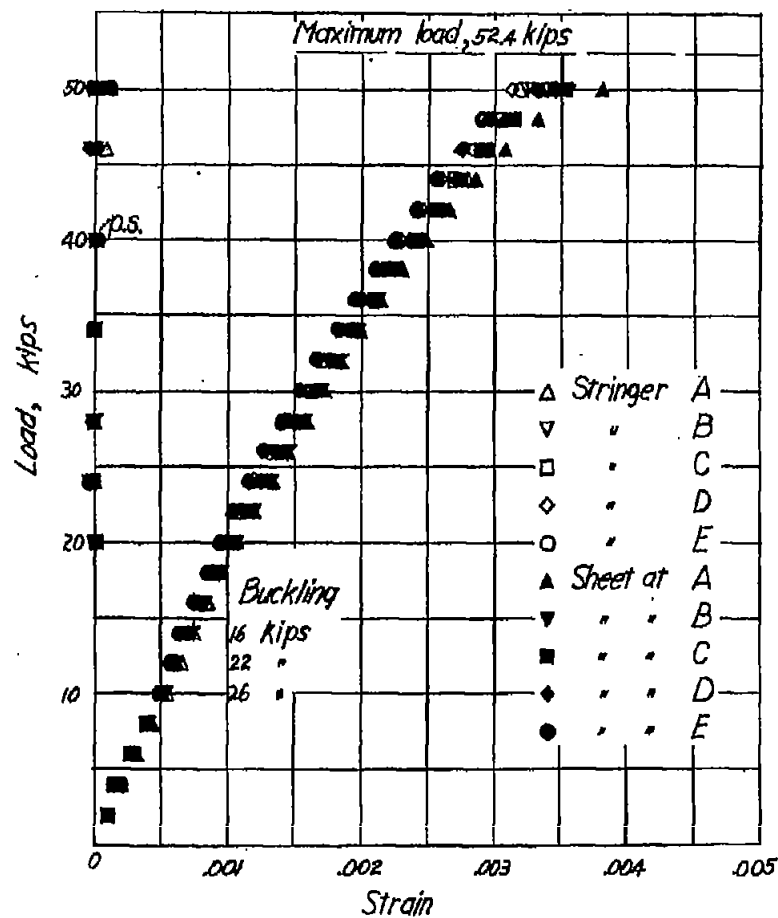


Figure 33.- Test of panel 24. No lateral pressure; length, 19 inches; sheet thickness, 0.0258 in.



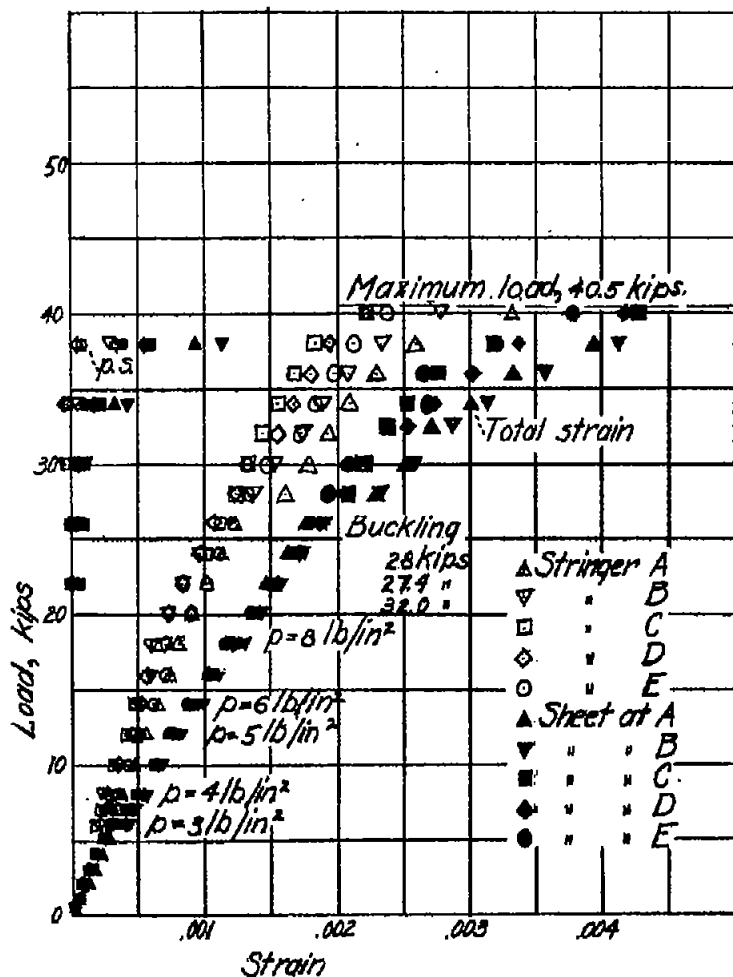


Figure 34.- Test of panel 25. Pressure on sheet side, 8 psi; length, 18 inches; sheet thickness, 0.0521 in.

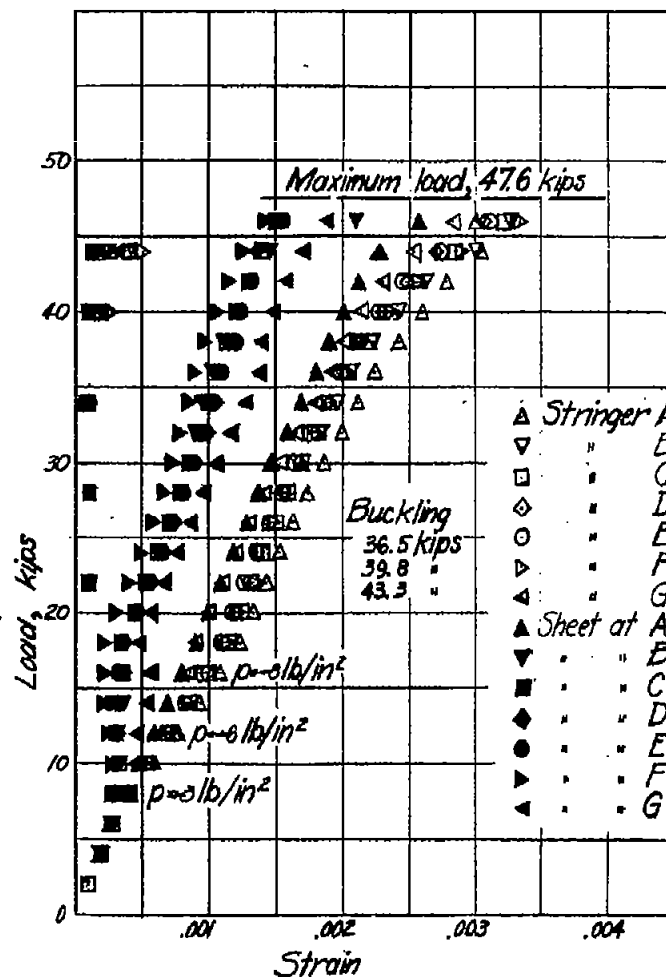


Figure 35.- Test of panel 28. Vacuum on sheet side, 8 psi; length, 18 inches; sheet thickness, 0.0359 in.

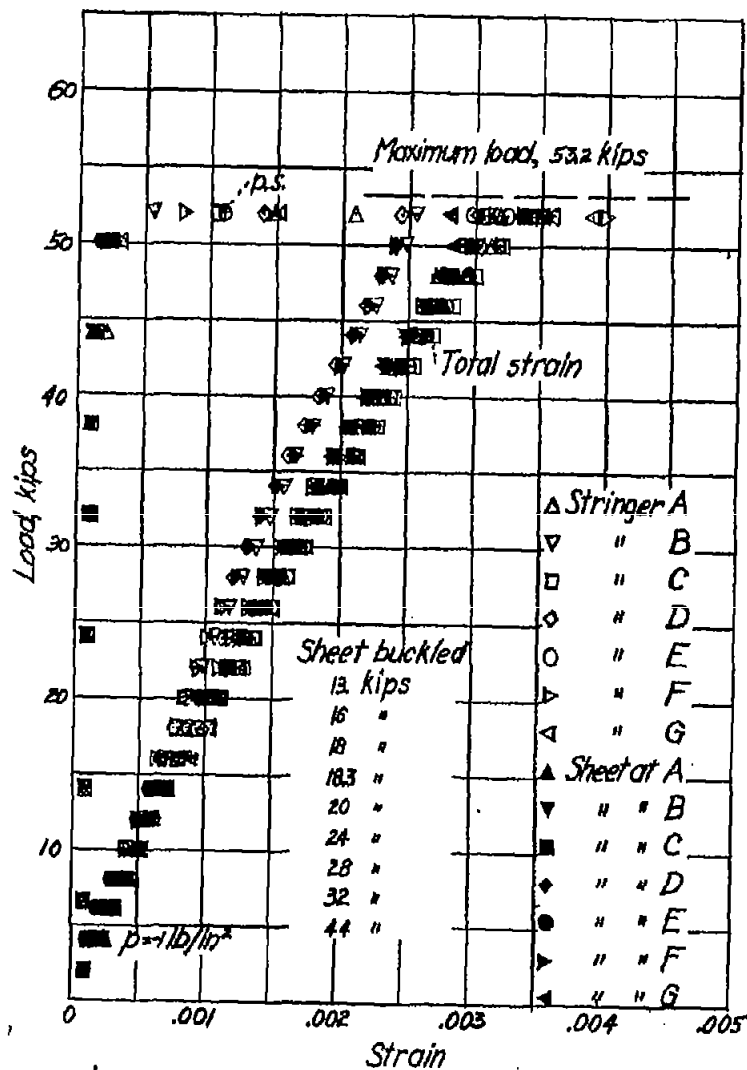


Figure 38.- Test of panel 27. Vacuum on sheet side, 1 psi; length, 19 inches; sheet thickness, 0.0262 in.

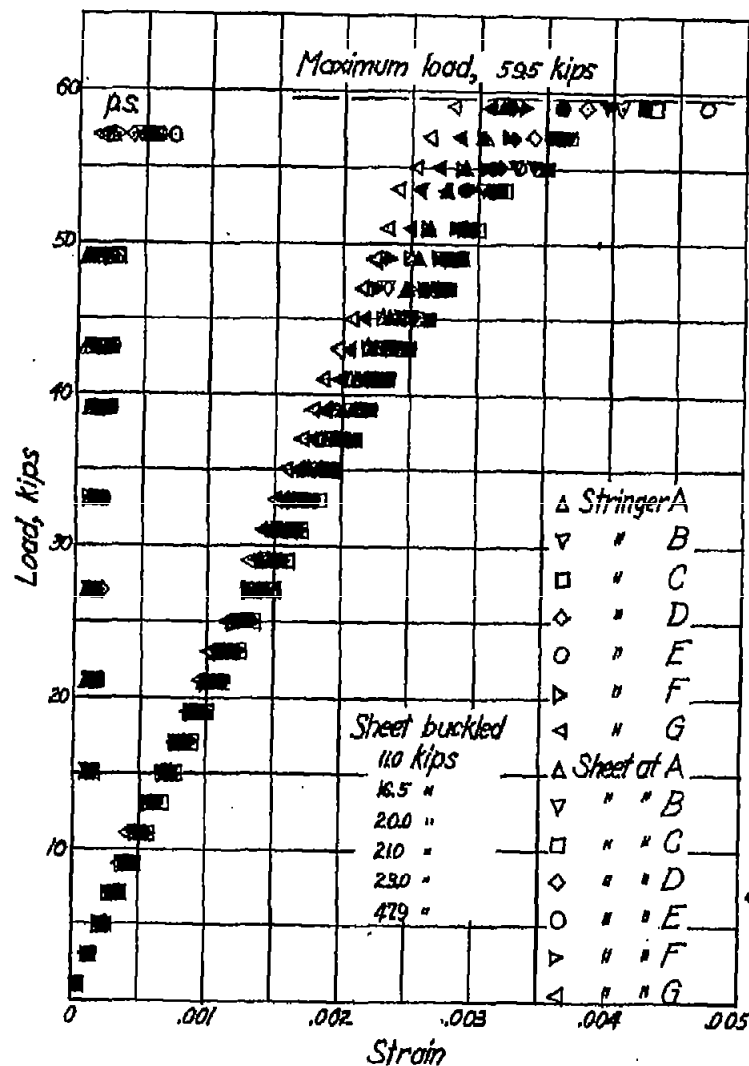


Figure 37.- Test of panel 28. No lateral pressure; length, 19 inches; sheet thickness, 0.0259 in.

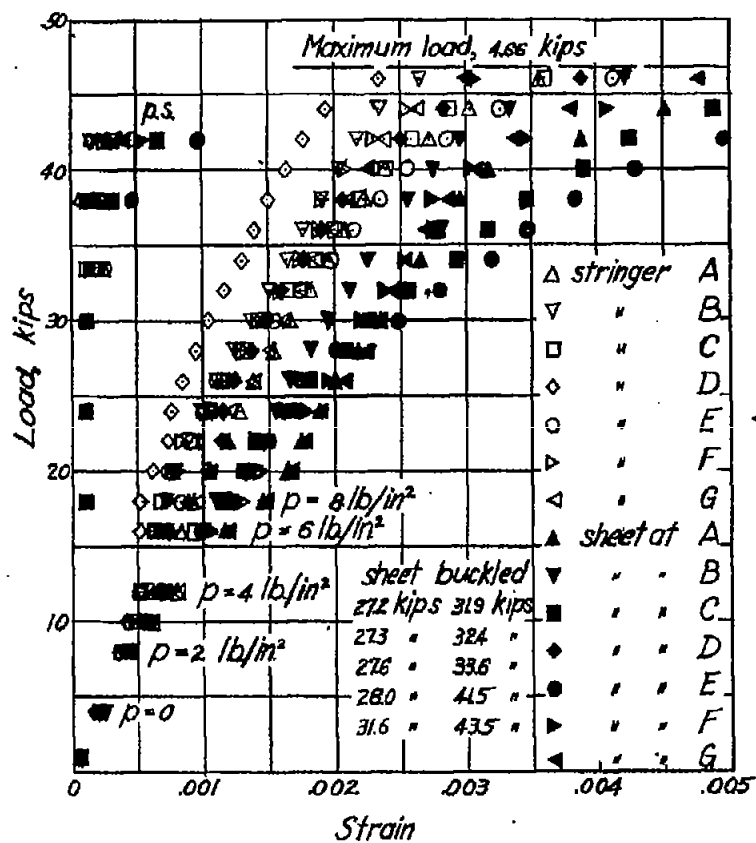


Figure 38.- Test of panel 39. Pressure on sheet side, 8 psi; length, 19 inches, sheet thickness, 0.0258 in.

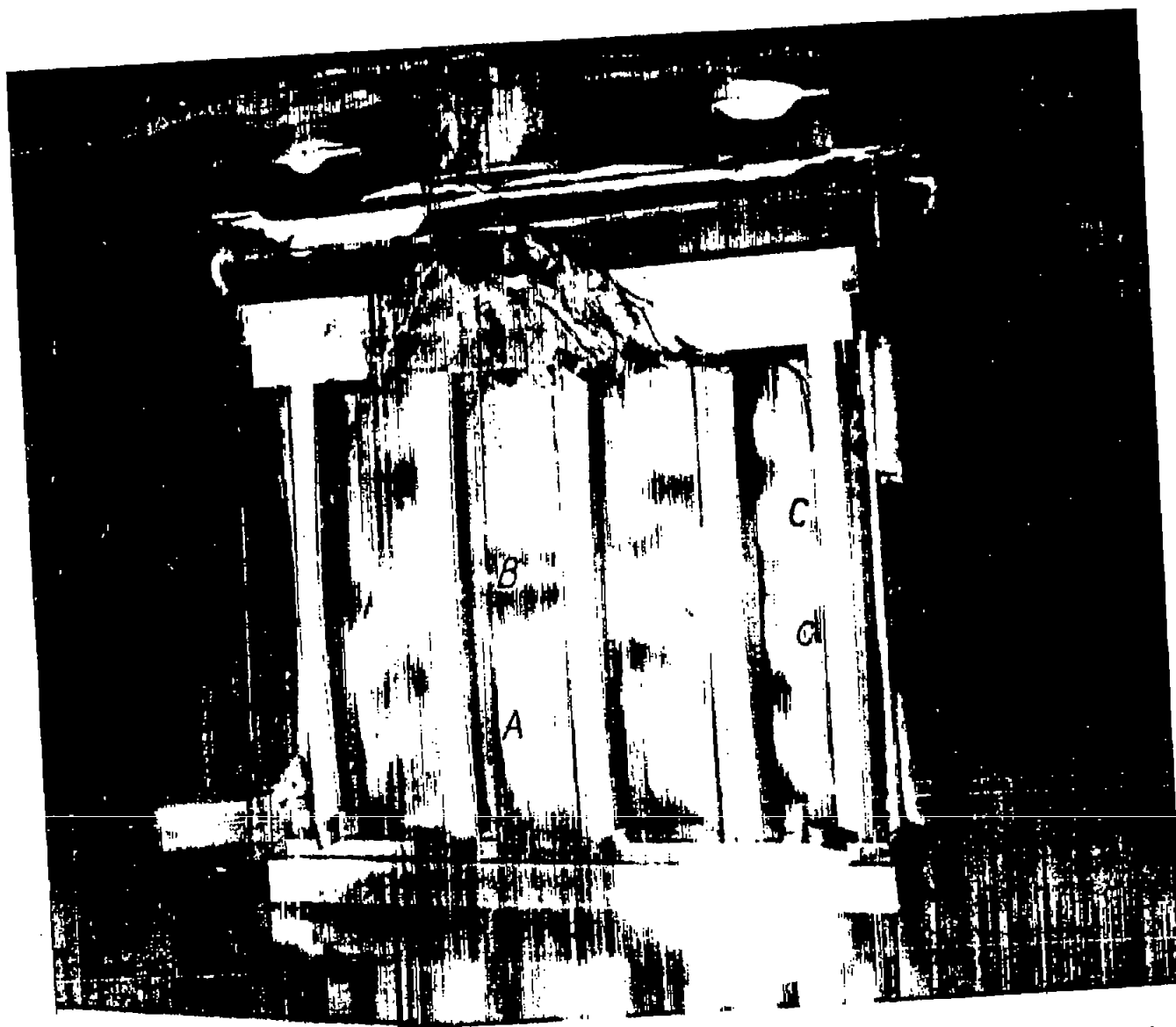


Figure 39.- Deflection of sheet under combined axial load and lateral pressure. At A, unbuckled sheet; at B, buckling from stringer; and at C, buckling only part way from stringer to stringer.

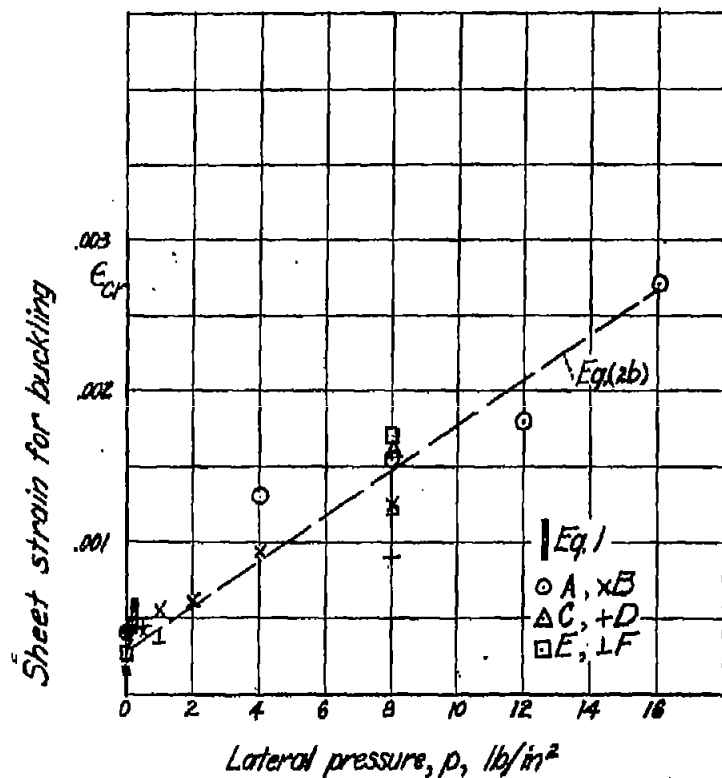


Figure 40.- Effect of lateral pressure on sheet strain at stringer edge for buckling of 0.026 inch panels. A and B, panels with pressure and vacuum on sheet side respectively for  $l = 12$  in.,  $w = 16\text{-}3/4$  in.; C and D the same for  $l = 19$  in.,  $w = 16\text{-}3/4$  in.; E and F the same for  $l = 19$  in.,  $w = 24\text{-}3/4$  in.

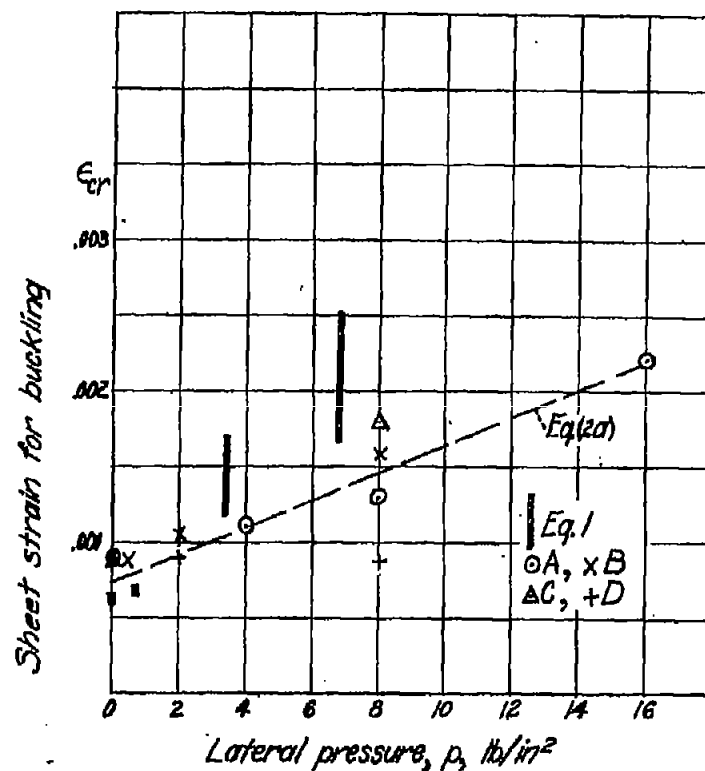


Figure 41.- Effect of lateral pressure on sheet strain at stringer edge for buckling of 0.051 inch panels. A and B, panels with pressure and vacuum on sheet side respectively for  $l = 12$  in.,  $w = 16\text{-}3/4$  in.; C and D the same for  $l = 19$  in.,  $w = 16\text{-}3/4$  in.

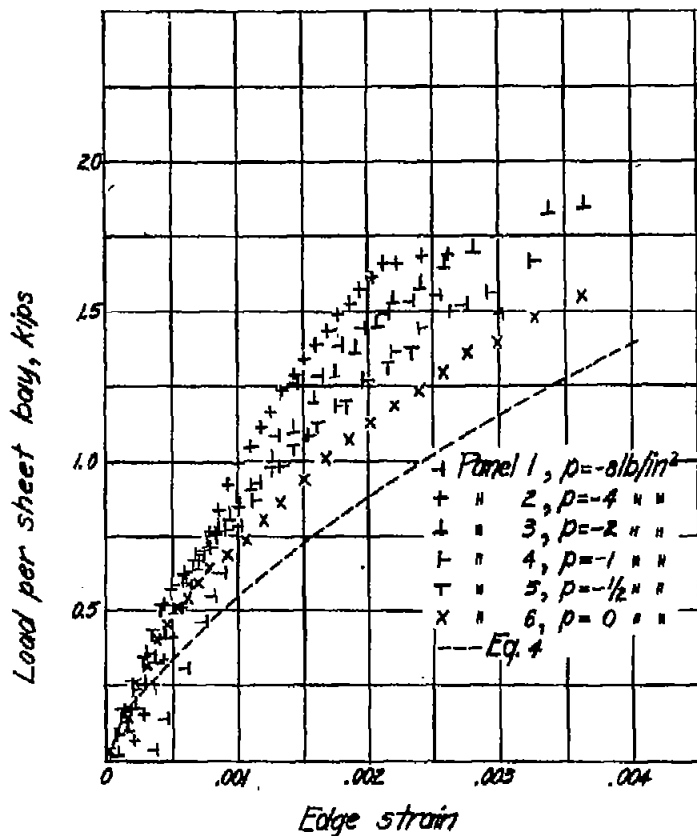


Figure 42.- Axial load carried per sheet bay for panels 1 to 6 with nominal 0.025 inch sheet, 4 inch stringer spacing. (Negative pressures, p, indicate vacuum on sheet side of panel.)

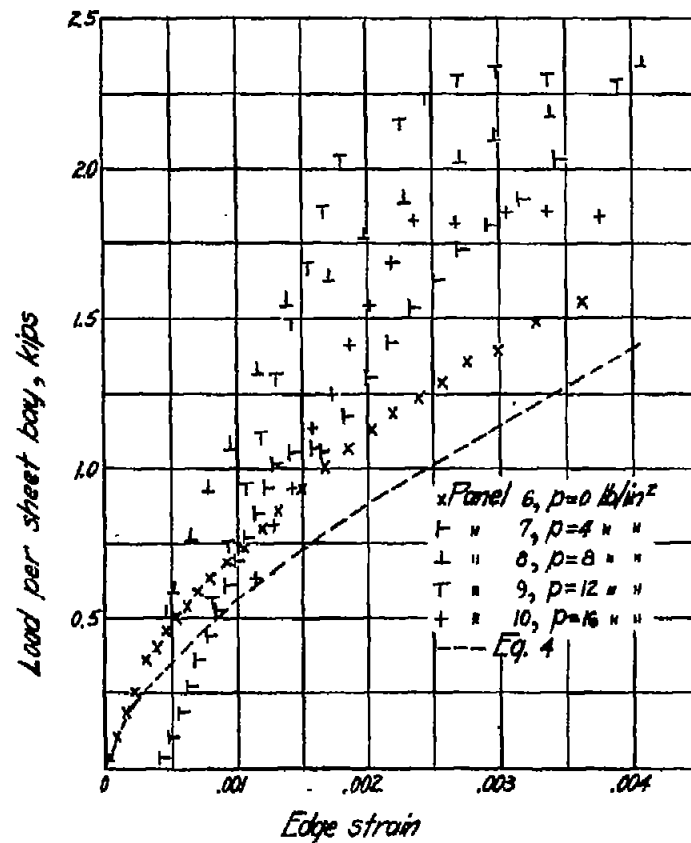


Figure 43.- Sheet load against edge strain, pressure on sheet side; length, 12 in.; sheet thickness, 0.025 in.

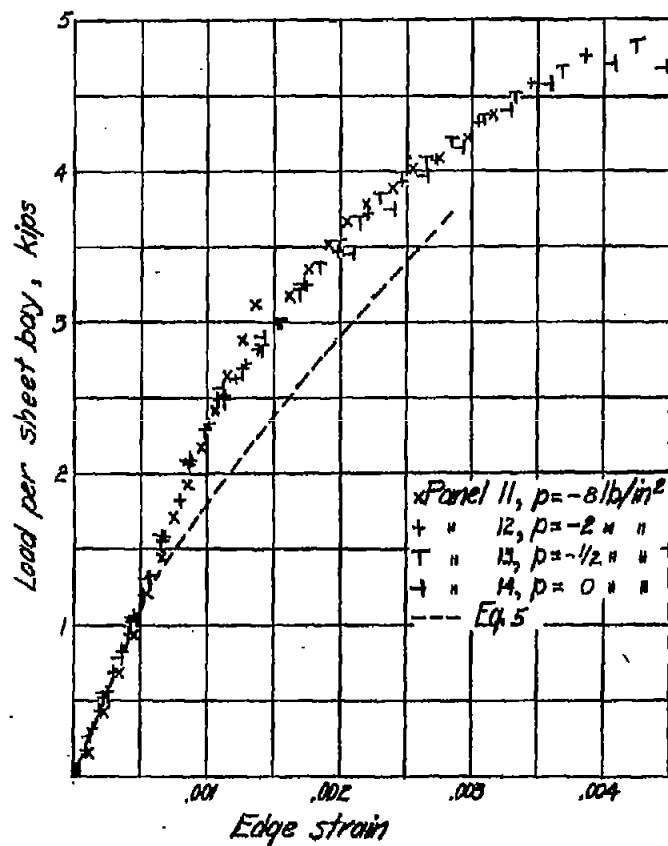


Figure 44.- Sheet load against edge strain; vacuum on sheet side; length, 13 in.; sheet thickness, 0.051 in.

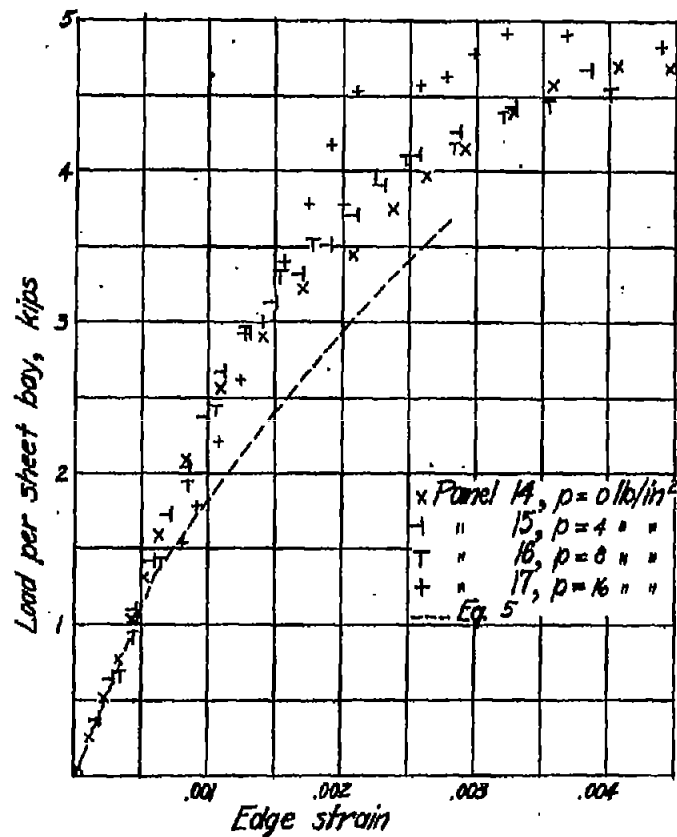


Figure 45.- Sheet load against edge strain; pressure on sheet side; length, 12 in.; sheet thickness, 0.051 in.

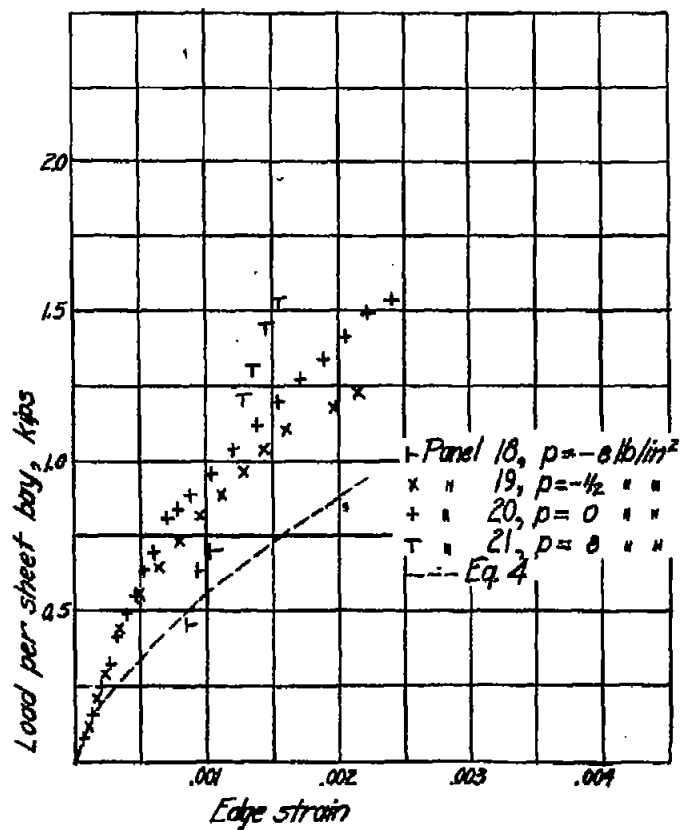


Figure 46.- Sheet load against edge strain; vacuum on sheet side; length, 19 in.; sheet thickness, 0.026 in.

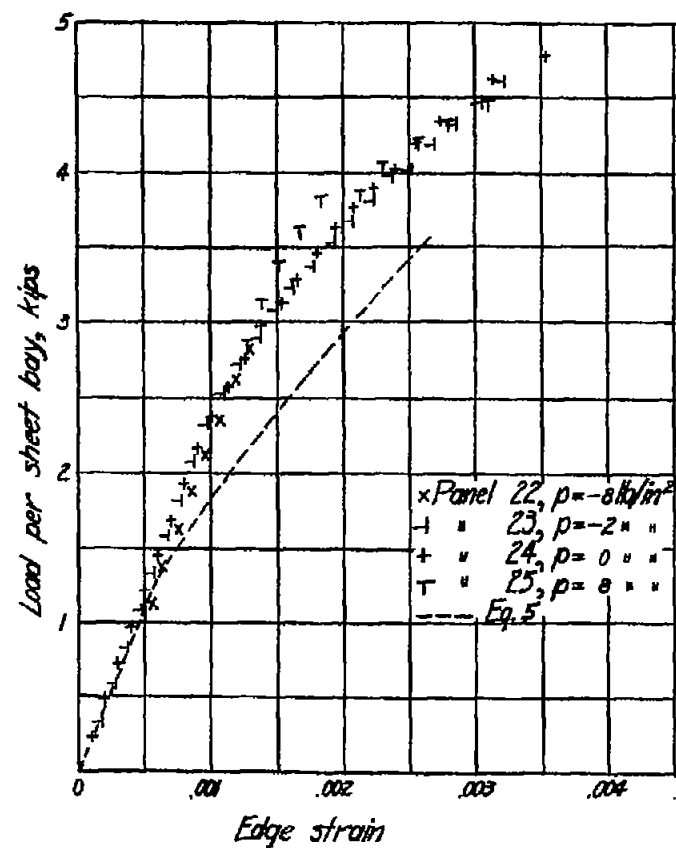


Figure 47.- Sheet load against edge strain; vacuum on sheet side; length, 19 in.; sheet thickness, 0.051 in.



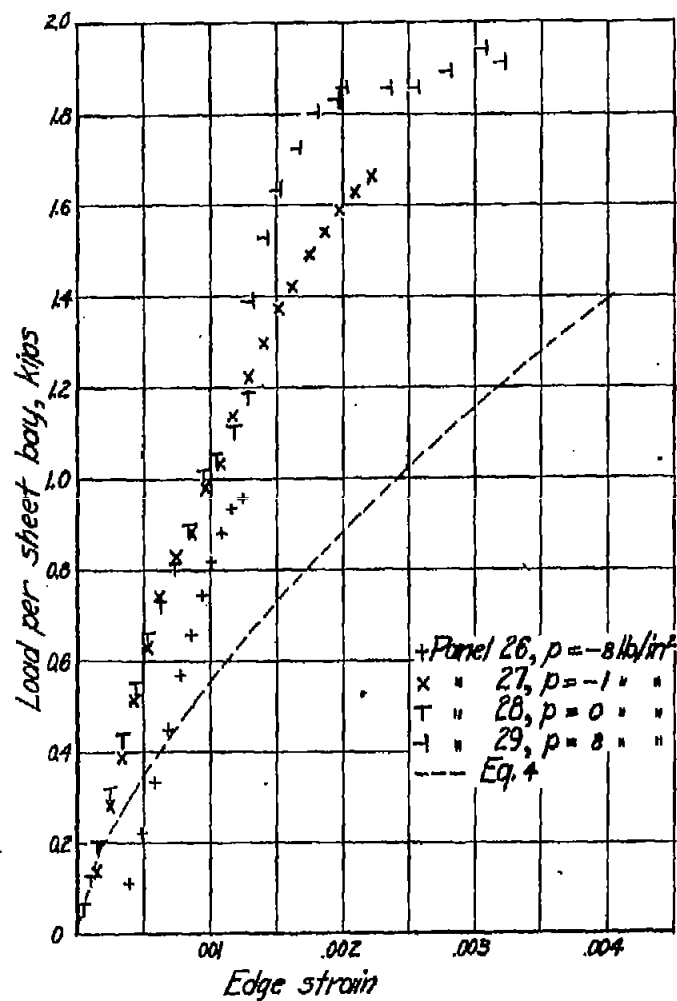


Figure 48.- Sheet load against edge strain; lateral load as indicated; length, 19 in.; six sheet bays; sheet thickness, 0.025 in.

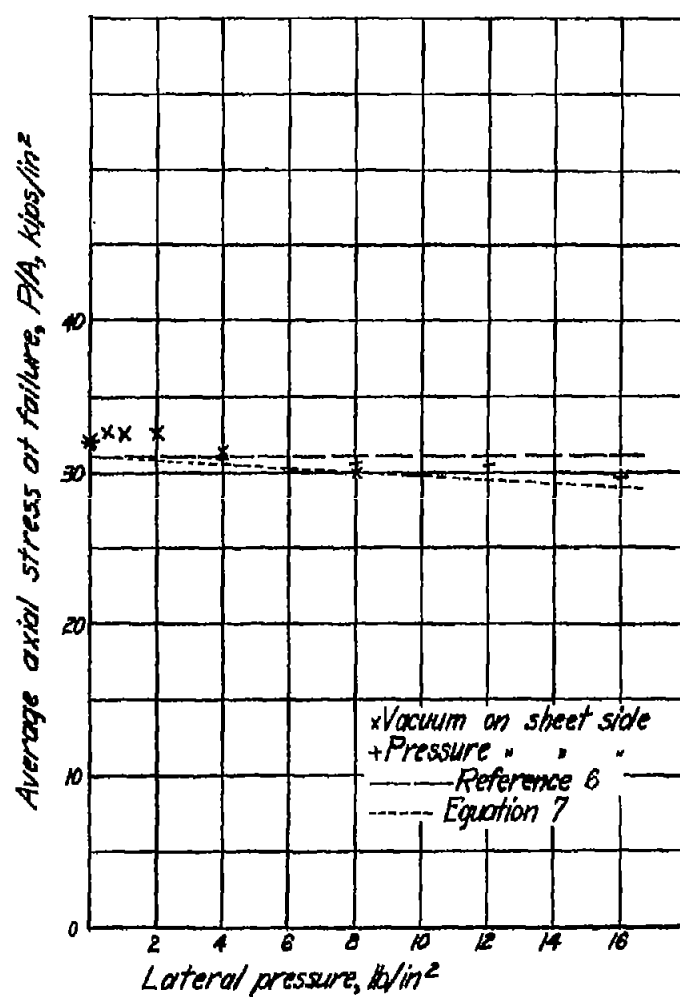


Figure 49.- Effect of lateral pressure on average axial stress at failure for panels 1 to 10 with 12 in. length and 0.025 in. sheet.

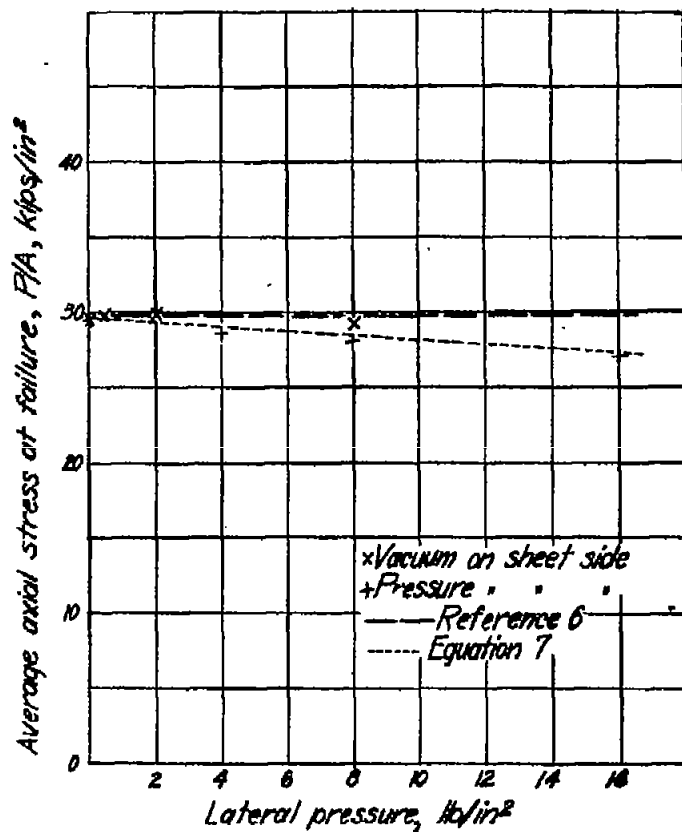


Figure 50.- Effect of lateral pressure on average axial stress at failure for panels 11 to 17 with 13 in. length and 0.051 in. sheet.

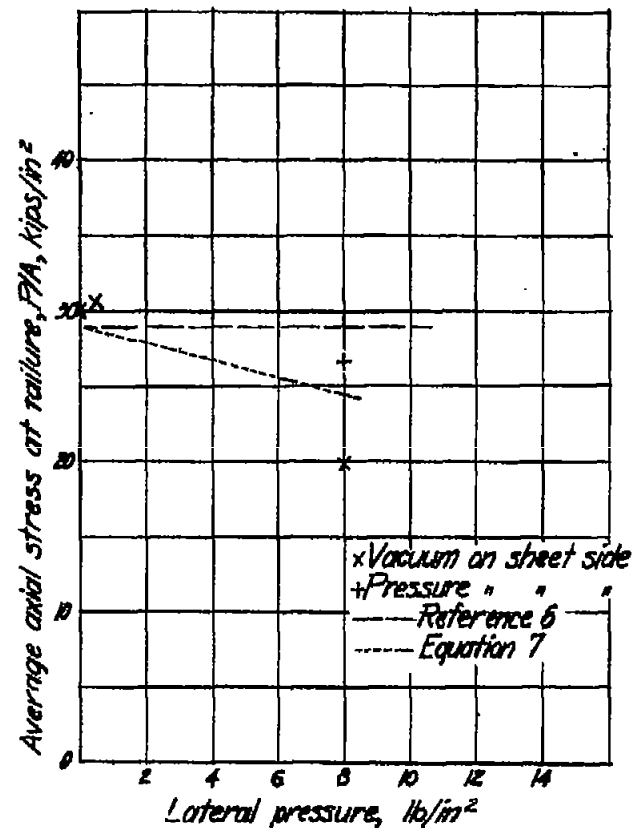


Figure 51.- Effect of lateral pressure on average axial stress at failure for panels 18 to 21 with 19 in. length and 0.035 in. sheet.

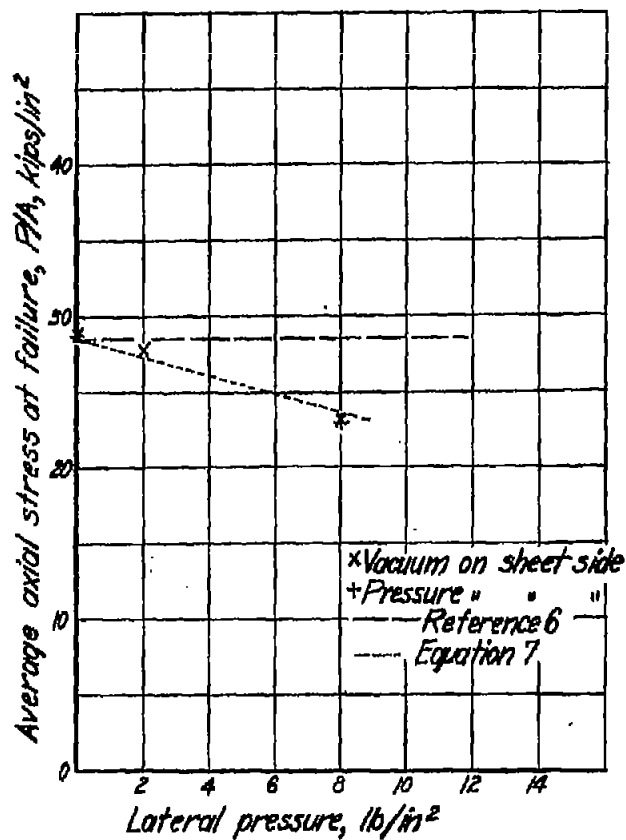


Figure 52.- Effect of lateral pressure on average axial stress at failure for panels 23 to 25 with 19 in. length and 0.061 in. sheet.

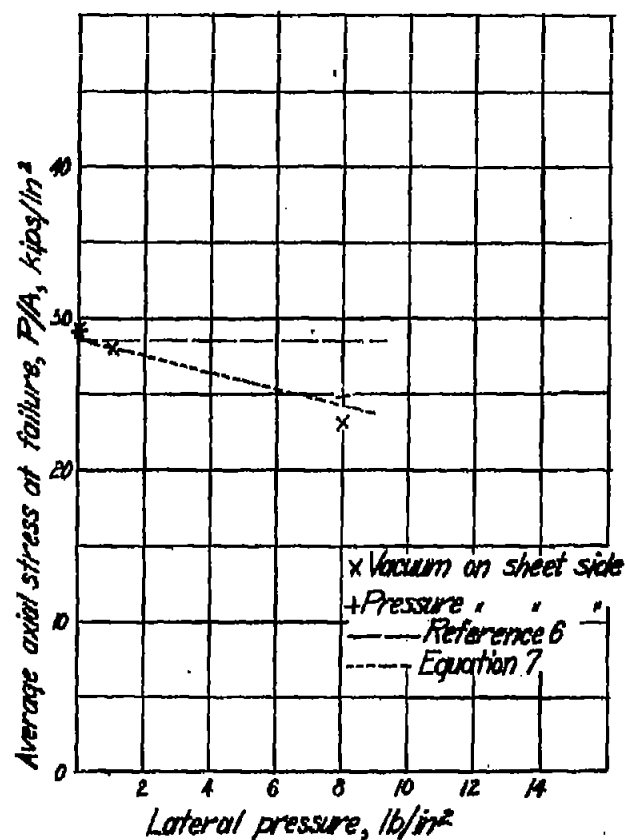


Figure 53.- Effect of lateral pressure on average axial stress at failure for panels 26 to 28 with 19 in. length; six sheet bays; 0.085 in. sheet.